2017

Voltage Regulation of Low Voltage Distribution Networks

Manisha Maharjan
South Dakota State University

VOLTAGE REGULATION OF LOW VOLTAGE DISTRIBUTION NETWORKS

BY

MANISHA MAHARJAN

A thesis submitted in partial fulfillment of the requirements for the

Master of Science

Major in Electrical Engineering

South Dakota State University

2017

VOLTAGE REGULATION OF LOW VOLTAGE DISTRIBUTION NETWORKS

MANISHA MAHARJAN

This thesis is approved as a creditable and independent investigation by a candidate for the Master of Science in Electrical Engineering degree and is acceptable for meeting the thesis requirements for this degree. Acceptance of this thesis does not imply that the conclusions reached by the candidates are necessarily the conclusions of the major department.

Reinaldo Tonkoski, Ph.D.

Thesis Advisor Date

Steven Hietpas, Ph.D.

Head, Electrical Engineering and Computer Science Date

Dean, Graduate School Date

ACKNOWLEDGEMENTS

I would first like to thank my thesis advisor Dr. Reinaldo Tonkoski of the Department of Electrical Engineering and Computer Science at South Dakota State University. I really appreciate his efforts for providing me continuous guidance and advice. He consistently allowed this thesis to be my own work, but steered me in the right direction whenever he thought I needed it.

I would also like to acknowledge Dr. Timothy M. Hansen as the second reader of this thesis, and I am grateful to him for his valuable comments on this thesis. I would also like to thank Dr. Zhen Ni and Dr. Robert Fourney who were involved in my thesis review and provided me fruitful suggestions. I would also like to acknowledge Dr. Douglas Malo for serving as my graduate faculty representative.

Beside my advisors and committee members, I am immensely grateful to Ujjwol Tamrakar for closely advising me in this thesis. I could have never completed this thesis without his thoughtful suggestions and insights. Also, I am very thankful to Dipesh for encouraging me in this work. I am overwhelmed to get support from my friends: Prajina, Abhilasha, Jharna, Naresh, Shiva, Mahesh, Bijen, Labi, Ayush, Venkat, Shuva and Fernando. Also, I am obliged to Mukesh for his motivation.

Finally, I must express my very profound gratitude to my guardians and family for providing me with unfailing support and continuous encouragement throughout my years of study and through the process of researching and writing this thesis. This accomplishment would not have been possible without them. Thank you.

Manisha Maharjan

CONTENTS

ABBREVIATIONS

AC	Alternating current
ADP	Adaptive dynamic programming
APC	Active power curtailment
DAB	Dual active bridge
DC	Direct current
DG	Distributed generation
ESS	Energy storage system
GW	Gigawatts
kVA	kilo volt-ampere
kW	kilowatts
LV	Low voltage
OLTC	On-load tap changer
PLL	Phase locked loop
POC	Point of connection
PV	Phototvoltaics
RES	Renewable energy source
SST	Solid state transformer
STATCOM	Static synchronous compensator
SVC	Static var compensator
VAr	Volt-ampere reactive

LIST OF FIGURES

LIST OF TABLES

ABSTRACT

VOLTAGE REGULATION OF LOW VOLTAGE DISTRIBUTION NETWORKS

MANISHA MAHARJAN

2017

The modern voltage distribution systems consist of distributed generation (DG), like photovoltaics (PV) and wind. These resources are inexhaustible and environmentally friendly. The existing low voltage (LV) distribution networks are typically designed for unidirectional power flow. The integration of DG makes the LV distribution networks prone to difficulties related to voltage, frequency, and power quality. The main challenges in the integration of DG occur due to the intermittent nature of DG. The amount of DG compared with the total generation resource on a power system network is measured as penetration. The system undergoes through reverse power flow when there is a high penetration of DG and low loading conditions in the network. The reverse power flow in the network negatively affects the voltage profile of the LV distribution networks. Thus, voltage regulation is required in LV distribution networks for the integration of DG.

Solid State Transformers (SSTs) are power electronic-based transformers that will be a vital component of the future smart grid. The future smart grid will have numerous DG which will require improved controllability to maintain proper coordination between stochastic DG and load. Among its various unique features, the reactive power compensating capabilities of SSTs can be explored in modern distribution systems for voltage regulation under high DG penetrations. SSTs are power electronic devices that show fast and non-linear dynamics which means the simulation models are often

complicated and need small time steps for accurate solutions. This prevents real-time and long-term simulation of large distribution systems as the simulations become computationally prohibitive. This work designs a simplified equivalent model of an SST using simple current and voltage sources along with simple modeling equations. These simplified models can be used to perform long-term voltage regulation studies of distribution systems where traditional transformers are replaced with SSTs.

Clean energy incentives and the continuous fall in the cost of PV installations have led to a steady growth in residential PV systems. One of the main consequences of higher PV penetration in LV distribution networks is the overvoltage problem. Active power curtailment (APC) of PV inverters has been previously used to curtail the output power of the inverters below its operating point to prevent such overvoltages. However, APC uses a constant droop-based approach to curtail the power, based on the difference between the measured voltage and a critical voltage level. In this thesis, APC is implemented with constant droop and other droop models in a typical LV distribution network in North America, with high PV penetration level. The simulation results show that the system undergoes excessive curtailment resulting in unnecessary energy loss. An adaptive droop-based approach using adaptive dynamic programming (ADP) is proposed as a possible solution to minimize the total energy loss in the system while keeping the system voltage under the critical operating limits. The energy loss due to curtailment decreased by 17.4% after implementing the adaptive-droop based approach using ADP.

CHAPTER 1 INTRODUCTION

1.1 Background

Renewable energy contributed an estimated 23.7% of global electricity by the end of 2015 [1]. The significant growth in the usage of renewable energy is the outcome of its never exhausting fuel and environmental concerns for producing little or no waste products such as carbon dioxide or other chemical pollutants. Among various renewable energy sources (RESs) available, solar energy is the cleanest and the most abundant source. Due to the global concern for clean energy and the drastic cost reduction in photovoltaics (PV) technology, the rise in the installation of PV is noteworthy over the last decade. About 227 gigawatts (GW) of PV installations contributed more than 1.3% of the world electricity supply at the end of 2015 [2].

Mainly, there are three major PV installation types in the market: residential rooftop, commercial plant, and utility-scale system [3]. Residential systems are usually few kilowatts in size, while the commercial and utility systems are generally in megawatt scale. The utility-scale systems are produced and distributed in the utility level of the electricity market. Generally, the residential systems are installed in households of low voltage (LV) distribution feeder in the form of distributed generation (DG). The integration of RES like residential PV in LV distribution feeders helps in addressing the energy demand without the addition of large generation and transmission units, that requires long periods of construction period and massive cost. Fig. 1.1 shows the annual residential PV installation for the past and upcoming years, indicating that the residential PV market has been growing rapidly due to the decrease in the installation cost. The

modeled cost to install PV systems for the residential sector decreased by 6% in 2016 compared to the previous year [4].

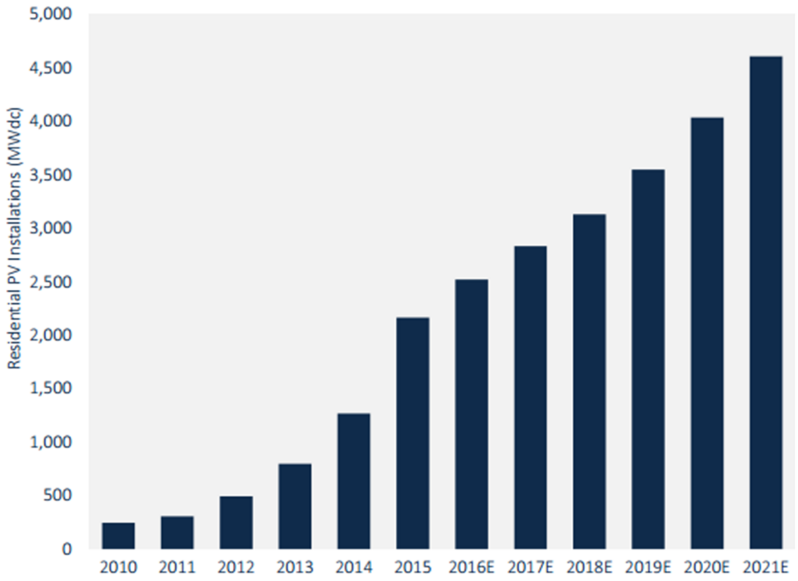

Figure 1.1. Annual residential PV installation PV forecast [5].

Traditionally, LV distribution networks are constructed for unidirectional flow of real power from the distribution transformers to the loads in the feeder. The protection schemes and control are available with regard to this unidirectional flow of power. With the integration of DG, the power is injected back into the grid. The reverse power flow in LV distribution networks increases the voltage at the point of connection (POC) [6]. This leads to the problems related to power quality and reliability of the system and consequently limits the capacity of DG installation. Power quality is an important measure that needs to be maintained by utility companies for their customers. They must guarantee the electricity supply for their customers while fulfilling certain quality requirements. The power quality may affect the end users, equipment and system manufacturers, and plant installations. The variation in voltage, frequency, and harmonics

are the most common challenges related to power quality during the integration of DG [7]. This thesis is directed towards the challenges due to the voltage change in the system due to the high penetration of intermittent DG and possible solutions. Voltage variation affects the operation and reliability of the power system. Hence, the voltage needs to be maintained within certain limits. Voltage regulation is the ability of the system to maintain its voltage constant in various load conditions.

One of the challenges that arises during high PV penetration and low loading condition in voltage regulation is voltage rise and if it exceeds a specified limit, it is termed as overvoltage. To avoid overvoltage, generally, PV power is curtailed, which results in loss of cheap and clean renewable energy. As the amount of curtailment increases, the economic and environmental benefits from PV installations decreases. Hence, LV distribution networks need to evolve to accommodate the increased PV penetration so as to get maximum benefits from it. These discussions highlight the need for the protection schemes and control at both the distribution and the DG connection points. Also, the power electronic components in DG can support voltage regulation of the distributed network.

1.2 Motivation

Voltage regulation is required for integrating DG like PV systems in LV distribution networks to maintain the power quality of the system. The control schemes at both the distribution level and the POC of DG are needed for maintaining the voltage standards and for maximum utilization of available energy.

1.3 Objective

The objective of this thesis is to develop strategies to maintain the voltage at the distribution level and at the point of PV system integration within acceptable limits, while maximizing the PV power injection in the network.

1.4 Contributions

The main contributions of this thesis are listed below:

(a) Developed and validated simplified equivalent model of solid state transformer (SST) with the average model of solid state transformer for voltage regulation studies of low voltage distribution systems.

(b) Compared quadratic and exponential droop models with constant droop value in current active power curtailment (APC) method to understand the effect of changing the droop value for curtailment minimization.

(c) Developed and implemented adaptive droop method to minimize the total energy loss due to power curtailment while keeping the system voltage under critical operating limits.

1.5 Thesis outline

This thesis has been organized as follows:

Chapter 2 comprises of the detailed description of the development of the equivalent model of the SST. The detailed process of the modeling along with the simulation results for verification of the model are presented in this chapter.

Chapter 3 describes APC and the quadratic and exponential droop models employed in APC method. The preliminary simulation results are presented for the three methods of

implementing voltage droops for APC. Moreover, it describes the drawback regarding APC method through illustrations with the simulation results. Further, this chapter proposes a supplementary droop adjustment for APC using adaptive dynamic programming. The proposed technique is evaluated using a simulation model of a twelve-house distribution system [8] and the results are analyzed and summarized.

Lastly, Chapter 4 presents the conclusions and the possible future work related to the research.

CHAPTER 2 EQUIVALENT MODEL OF SOLID STATE TRANSFORMERS FOR VOLTAGE REGULATION STUDIES

2.1 Introduction

Residential PV installations have seen a steep rise in recent years due to the high demand for renewable clean energy and the ever decreasing cost of PV systems. PV growth at the distribution level has surged forcing the utilities to upgrade their operating mechanisms to ensure power quality and reliability. This has been highlighted by the various changes proposed to the IEEE 1547 standard regarding reactive power compensation and voltage regulation [9]. One of the major challenges due to the high penetration of DG has been in the voltage regulation of the distribution systems. The lack of proper control and protection often limits the installation of these DG sources in the distribution network.

Various technologies exist in the literature that aims at solving the issues of voltage regulation, like using on-load tap changers (OLTCs), voltage regulators, energy storage, APC, and/or reactive power compensation from DG units. Dedicated reactive power compensating devices, like Static Var Compensator (SVCs) and Static Synchronous Compensators (STATCOMs), have also been widely employed for reactive power compensation [8], [10]. With recent advancements in wide-bandgap semiconductor technology and the reduced cost of switching devices, SSTs will be a core component of the future smart grid [11]. SSTs can give higher efficiency and a higher degree of controllability than conventional transformers because of the presence of wide-band gap semiconductor switches which have lower switching losses. SSTs with reactive power

compensation capabilities will have a major influence in the voltage regulation of the future smart grid with high renewable energy penetration [12]. SSTs are power electronic devices comprised of switching converters for producing desired conversion and control functions. The number and type of switching converters depend on the topology of the SST. The high frequency switching mechanisms involved in SSTs make the models and controllers of these systems often complicated and computationally intensive to simulate and solve. The time-step required for the simulation has to be smaller than the switching frequency and is often in the range of microseconds. Although these simulations are able to capture the dynamic and steady-state behavior of the system, the model is overly complex for voltage regulation studies. Moreover, the simulations using such detailed models are complex and cannot be used to perform real-time simulations and long-term analyses. The high frequency dynamics are not important for system level steady-state studies of distribution systems [13]. Instead, real-time simulations which model the desired system behavior are needed. The task becomes even more complex when performing long-term simulations. Hence, there is a need for simplified equivalent models of the SSTs which model the main functionalities of an SST.

2.2 Previous Work

Research on SSTs has increased since there is a major concern to enhance the functionality and efficiency of the conventional transformers in distribution systems connected to the grid. Ramchandran et al. [14] presented a detailed SST control based on average model that can be used for system level studies and distribution feeder protection studies. The SST presented demonstrated bidirectional power flow ability and the ability

to respond under fault conditions. The model consists of a high-bandwidth controller and does not verify the functionality required for voltage regulation. Similarly, Mao et al. [15] developed a cycle-by-cycle average model to design the various control loops of the SST in view of simplifying the complex model of an SST. The model had high bandwidth control loops which would prevent real-time simulation of power systems with SSTs at the distribution system level. Jiang et al. [13] and Zhao et al. [16] developed the simplified average models which aim at removing these high bandwidth control loops for system level simulation under various assumptions. However, these models are still computationally complex for larger system level studies.

With the high penetration of DG (solar and wind plants) in distribution systems, the SST can be used for connecting the grid with the distribution systems instead of the conventional transformers. The challenges regarding the voltage regulation due to DG integration can be addressed using SST. She et al. [17] proposed a novel wind energy system with integrated SST that has an active power transfer, reactive power compensation, and voltage-conversion capabilities. The developed system suppressed the voltage fluctuation caused by the intermittent nature of wind energy without the use of STATCOMs. Moreover, the AC residential load can be integrated using the low voltage AC port of the SST [18]. Although there are many current research projects in progress to find the application of SST in voltage regulation studies, there is a need of simplified steady-state equivalent model of SST to explore the functionalities of SST in distribution networks.

2.3 Objective

The objective of this work is to design a simple equivalent model of an SST that can be used for long-term voltage regulation and other system level studies of the distribution networks. The designed model needs to represent all the main functionalities of an SST i.e., reactive power compensation, active power control, power factor control, bidirectional power flow control, and secondary voltage regulation.

In this work, simulations are performed in MATLAB/Simulink to test the proposed model and are verified against an average model presented by Zhao et al. [16]. The designed model can be used for voltage regulation studies using reactive power compensation capabilities for the distribution systems.

2.4 Solid State Transformer (SST)

SST is a power electronic implementation of a traditional transformer. A combination of power electronic devices and a high frequency transformer is used to achieve the same functions as that of a traditional transformer [19]. A typical topology of an SST, as shown in Fig. 2.1, connects high voltage bus with low voltage bus using power electronic components and high frequency transformer. The grid voltage is converted into a high frequency AC voltage through power electronic converters and then fed to the primary side of a high frequency transformer. The high frequency transformer reduces the volume and provides galvanic isolation for AC-AC conversion. The high frequency AC voltage is converted to lower voltage DC and the obtained voltage is finally converted to a 50/60 Hz low AC voltage using an inverter at the output. During these conversions, a high voltage DC bus and a low voltage DC bus are generated on the primary and secondary

side of the high frequency transformer. A regulated low AC voltage is achieved at the end of the SST configuration.

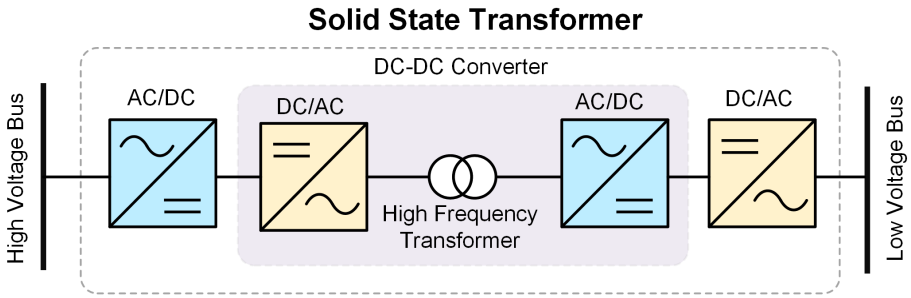

Figure 2.1. Schematic diagram of a typical solid state transformer.

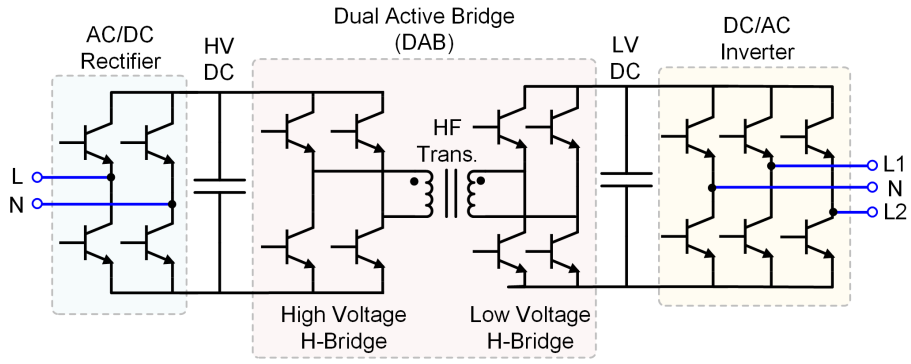

Figure 2.2. Detailed circuit diagram of a solid state transformer.

There are a number of existing topologies for SST [20]. Some of the basic configurations of SST are mentioned as: a) single-stage with no DC link, b) two-stage with low voltage DC links, c) two-stage with high voltage DC links, and d) three-stage with both HVDC and LVDC links. Among the various topologies, the three stage Dual Active Bridge (DAB) based topology, shown in Fig. 2.2, provides most of the functionalities of an SST with simplified control design. The SST includes an AC/DC rectifier that converts the input AC voltage to a high voltage DC. Then, a DAB converts this high voltage DC to a low voltage DC. Finally, the DC/AC inverter converts the low voltage DC to the desired low voltage AC on the secondary side. The AC/DC rectifier usually has an H-bridge

configuration with high voltage DC output. Active power factor correction techniques are implemented within this input rectifier to maintain unity power factor at the input side. The DAB consists of a high voltage and a low voltage H-bridge along with a high frequency transformer and controls the high voltage and low voltage DC links. The output DC/AC inverter controls the output AC voltage at two output ports of the SST.

SST is basically designed for transforming voltage from medium to high frequency isolation, thus leading to the advantage of reduced volume and weight when compared to traditional power transformer. The configuration of the SST allows various functionalities which can not be provided by the traditional power transformers. The presence of semiconductor switches and circuits allow possible regulation of voltage and current which enables SST for voltage sag compensation, fault current limitation, power flow control, etc. The converters in the secondary side of the SST facilitate a regulated DC bus, which enables direct regulated connection of DG and energy storage components like rooftop PV systems, wind turbine systems, natural gas generators and battery banks to DC microgrids. SSTs can offer reactive power support for the grid within limits of its rating for voltage regulation. SST facilitates desirable output ports in the system for integration of DC systems and AC systems which can be used in distribution systems and microgrids. Moreover, SSTs can increase controllability and flexibility of a system due to the presence of different power electronic converters in different voltage levels and forms. Additionally, SSTs can also be implemented for harmonic regulations, voltage sag compensation, power quality improvement, etc. [18], [19], [21].

2.5 Modeling of Solid State Transformer

Even though the average model of SST allows faster simulations compared to the detailed switching models, it is still complex due to the presence of various control loops. The control loops need to be tuned properly, which is not the main concern when it comes to system level studies. Thus, the complexity of the average model needs to be reduced so that a fairly simple model that functions as an SST during steady-state can be used for voltage regulation studies of distribution systems.

2.5.1 Assumptions and Limitations of Equivalent Solid State Transformer Model

The proposed simplified equivalent model of SST has retained all the main functional capabilities of a typical SST. To reduce the complexity of the model, some assumptions have been considered to derive the simplified mathematical model of SST. The list of assumptions is as follows:

(a) The low AC voltage on the secondary side of SST is constant at the set reference value. However, the reference value can be adjusted which may help in Volt/VAr control studies.

(b) Reactive power compensated by SST is set within limits depending on the kVA power rating of the SST and active power flow.

(c) The DC ports available in SST were neglected.

(d) Dynamic response of the SST has been neglected.

Hence, the simplified model designed in this paper has some limitations as to when it can be used and depends on upon the type of analysis being performed. Here, the main

motivation is to develop the model for the steady-state voltage regulation analysis of the distribution systems and the long-term analysis of such systems. For such simulations, the dynamics of the SST itself can be neglected without affecting the simulation results.

2.5.2 Solid State Transformer Modeling

As per above simplifications, the equivalent model of SST is introduced, as shown in Fig. 2.3. The primary side of SST is modeled as a controlled current source and the secondary side of SST is modeled as constant voltage sources in a 120/240V AC split phase configuration. The DC conversion of voltages and the frequency transformations of voltages are neglected, thus only the major step down of voltage from grid level to distribution level is replicated in this simplified equivalent model of SST.

Since an SST operates in specific points based on power factor and loading level, power loss can be modeled as equivalent SST resistance [22]. The values of resistance on two sides of SST vary as per the transformer loading and also due to the bidirectional power flow. For a simpler approach, the effect of power factor is neglected and assumed to be constant. The primary and secondary side equivalent resistance equations are obtained by fitting the resistance data from the review paper by Stefanski et al. [22] at unity power factor and 0.86 power factor respectively as shown in Eq. (2.1) and Eq. (2.2). Various curves with different functions were fitted using curve-fitting tool in MATLAB and the curves with the highest R-squared value were chosen. The fitted curves provide equivalent resistance on primary side $R_{pri,pu}$ and secondary side resistance $R_{sec,pu}$ as a function of the

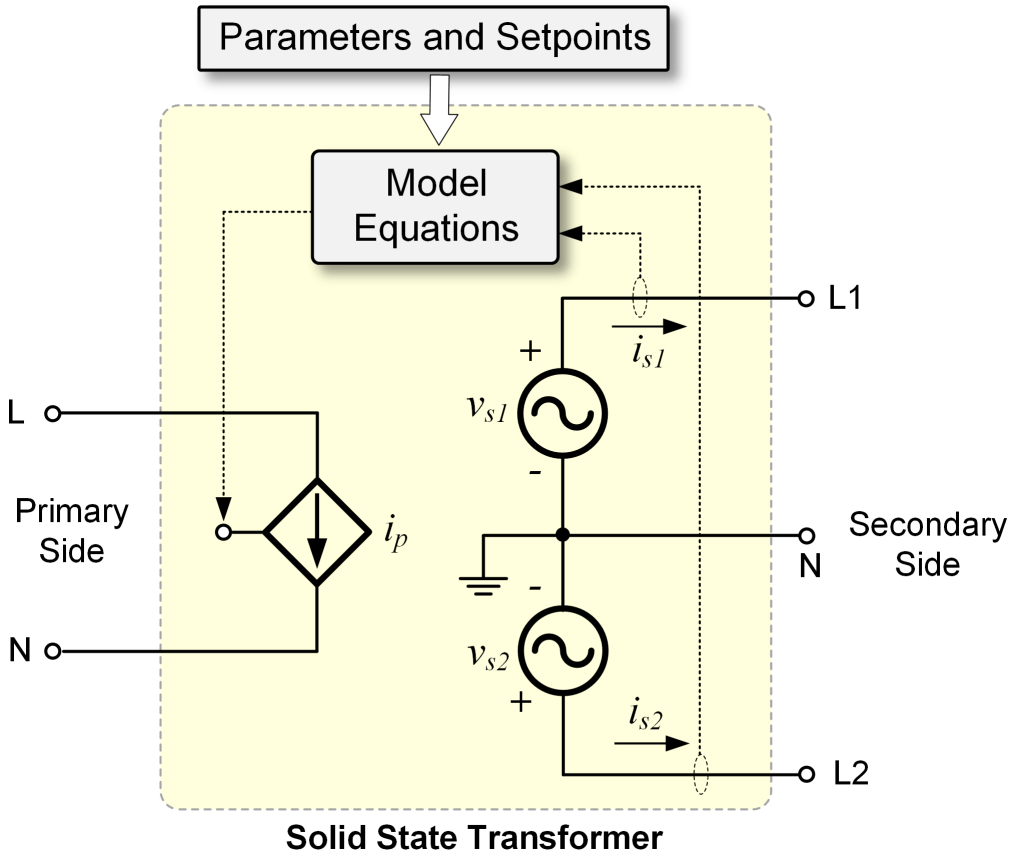

Figure 2.3. Equivalent model of a solid state transformer.

transformer loading as follows:

$$R_{pri,pu} = 0.0125x^{-1.410} + 0.0492 \tag{2.1}$$

$$R_{sec,pu} = 0.0038x^{-0.866} + 0.0012 \tag{2.2}$$

where x is the loading of SST as percentage of the transformer kVA rating. The loading of the SST can be calculated by

$$x = \left| \frac{P_L + jQ_L}{S_{rating}} \right| \tag{2.3}$$

where P_L and Q_L are the active and reactive power load on the SST, respectively, and

S_{rating} is the kVA rating of the SST. The modeled equations are developed in a per unit system so that it can be molded to any ratings of SST for future work. The secondary and primary side equations are modeled separately. The load demand and loss on the secondary side are first measured and the corresponding active and reactive power flows for the primary side are calculated including the losses. The total power demand on the secondary side $P_{sec,pu}$ in per-unit is calculated by

$$P_{sec,pu} = P_{L,pu} + I^2{}_{sec,pu} R_{sec,pu} \tag{2.4}$$

where I_{sec} is current flow in the secondary side of SST.

For the primary side modeling equations, the on-demand reactive power that can be compensated by SST are set within limits depending on the SST rating and secondary side active power flow. The series of equations to determine the primary side values are given below.

The total active power in primary side is given by

$$P_{total,pu} = P_{sec,pu} + \left| \frac{P_{sec,pu} + jQ^*{}_{grid,pu}}{V_{grid,pu}} \right|^2 R_{pri,pu} \tag{2.5}$$

Then the peak value of primary side current in per unit is given by

$$I_{pri,pu} = \frac{P_{total,pu} + jQ^*{}_{grid,pu}}{V_{grid,pu}} \tag{2.6}$$

Also, the phase of primary side current is calculated using

$$\phi = \arctan\left(\frac{Q^*_{grid,pu}}{P_{total,pu}}\right) \tag{2.7}$$

The instantaneous value of primary side current is given by

$$i_{pri} = \sqrt{2} I_{pri,pu} \sin(\omega t - \phi) \tag{2.8}$$

where $Q^*_{grid,pu}$ is the reference on-demand reactive power of grid, $V_{grid,pu}$ is the grid voltage, and ωt is the phase of grid voltage measured using a Phase Locked Loop (PLL).

2.6 Simulation Results

A 20 kVA SST with 7.2 kV, 60 Hz as single phase input voltage and 120/240V, 60 Hz split phase output is modeled for the simplified equivalent model. The simplified equivalent model of SST is simulated in MATLAB/Simulink and validated by comparing against the functional results of an average model of SST presented by Zhao et al. [16]. The model is tested under three cases to check its functionalities. The conditions for the tests are maintained same as in the average model of SST presented by Zhao et al. [16] for comparison. First, a load change test is performed to analyze how the model responds to load changes on the secondary side of the SST. Next, the bidirectional capabilities of the model were analyzed by adding a current source (representing a DG unit) connected to the secondary side. Finally, the reactive power compensating capabilities of the SST was also analyzed.

2.6.1 Load Change Condition

In this case, 6 kW loads were connected to each phase of the secondary side of the SST throughout the simulation. At a simulation time of 1 s, the active power load on phase 1 of the secondary side was increased from 6 kW to 9 kW along with a reactive power load increase from 0 kVAr to 5 kVAr, as shown in Fig. 2.4. The active and reactive power on phase 2 remained constant throughout the simulation at 6 kW and 0 kVAr respectively, as shown in Fig. 2.5. From Fig. 2.6, it can be observed that only the active power was transferred through the SST from the grid. The input reactive power remained zero throughout the simulation, only the active power has increased from 12.6 kW to 15.8 kW to supply the increased active power demand on the secondary side and the losses in the SST. The reactive power for the load was supplied only from the secondary side of the SST. The total power loss in the SST increased with the increased power demand, as shown in Fig. 2.7.

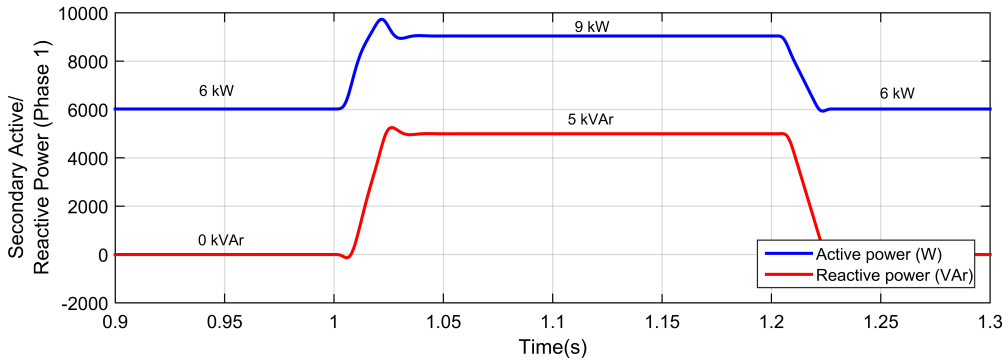

Figure 2.4. Active and reactive power of secondary side (Phase 1) of solid state transformer under load change.

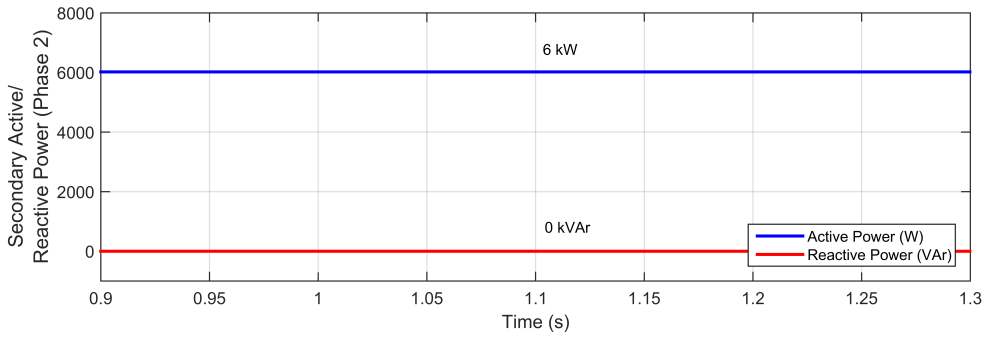

Figure 2.5. Active and reactive power of secondary side (Phase 2) of solid state transformer under load change.

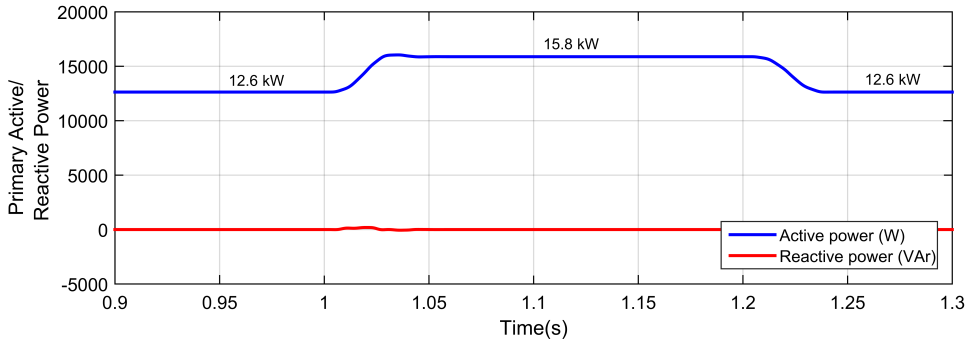

Figure 2.6. Active and reactive power of primary side of solid state transformer under load change.

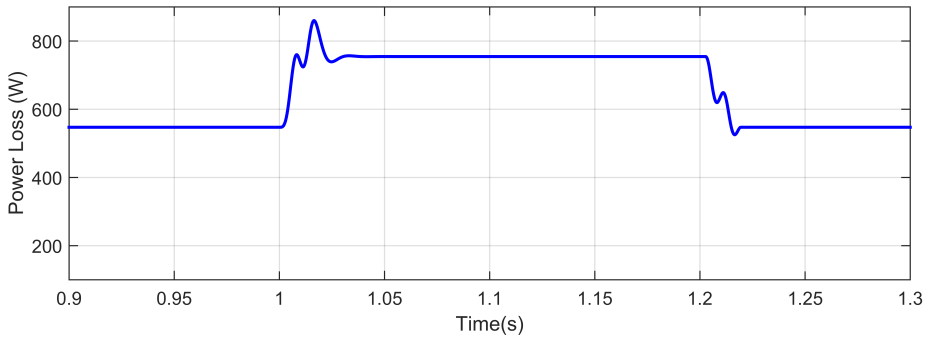

Figure 2.7. Total power loss in solid state transformer under load change.

Fig. 2.8 shows the voltage/current waveforms of phase 1 on the secondary side of the SST for the load change tests as described previously. The waveforms were initially in

phase but once the reactive load was added at a simulation time of 1 s, the current lagged the voltage indicating the secondary side was able to provide the reactive power demand of the load. The phase 2 secondary voltage and current waveforms, as shown in Fig. 2.9, were in phase throughout the simulation since only an active power load was connected. As the primary side does not transfer any reactive power, the voltage and the current waveforms were in phase and the primary side operated at unity power factor throughout the simulation as shown in Fig. 2.10. The response of the SST model designed here when subjected to load changes were similar to what was observed with the average model of the SST [16].

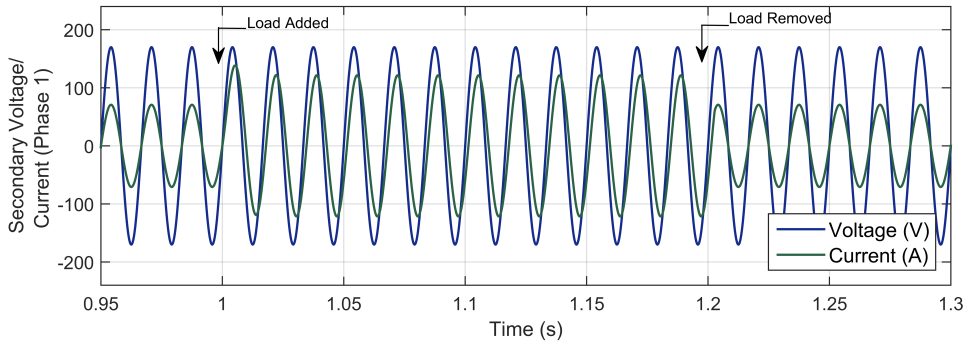

Figure 2.8. Secondary side (Phase 1) voltage/current waveforms of the solid state transformer under load change.

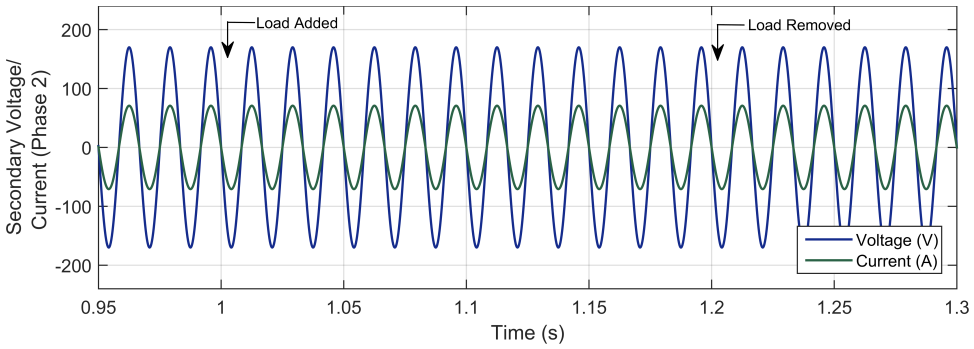

Figure 2.9. Secondary side (Phase 2) voltage/current waveforms of the solid state transformer under load change.

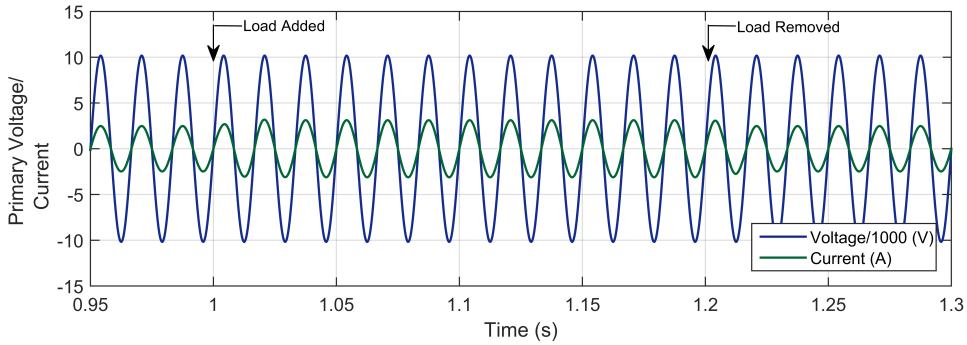

Figure 2.10. Primary side voltage/current waveforms of the solid state transformer under load change.

2.6.2 Bidirectional Operation Mode

In this case, the bidirectional power flow functionality of designed SST model was analyzed. A current source that would inject 10 kW of active power was added in both the phases of the secondary side to emulate a DG source, which could supply power back to the grid through the SST. As shown in Fig. 2.11 and Fig. 2.12, the active power of the secondary side of the SST on both phases decreased from 6.02 kW to -3.99 kW when the current source was added for simulation time of 2 s to 2.2 s. Likewise, the total active power on the primary side also changed from 12.06 kW to -7.66 kW for a simulation from 2 s to 2.2 s, as shown in Fig. 2.13, indicating that the power was being transferred from the secondary side of the SST to the primary side (or the grid). The primary side voltage and current waveforms were out of phase with each other when the active power was injected into the secondary side of SST, as shown in Fig. 2.14. Again, the results of the simplified model are comparable to the results achieved using the average model [16].

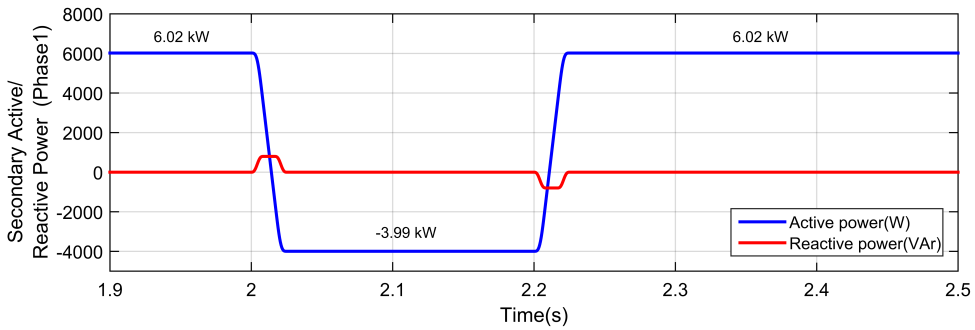

Figure 2.11. Secondary side (Phase 1) active and reactive power flows under bidirectional mode of operation.

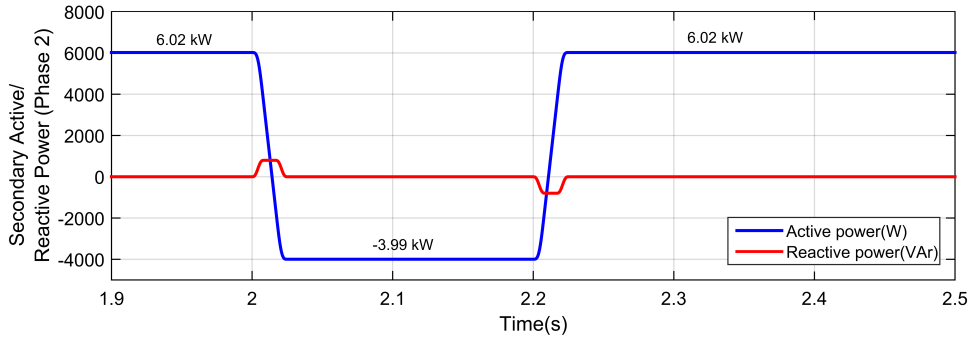

Figure 2.12. Secondary side (Phase 2) active and reactive power flows under bidirectional mode of operation.

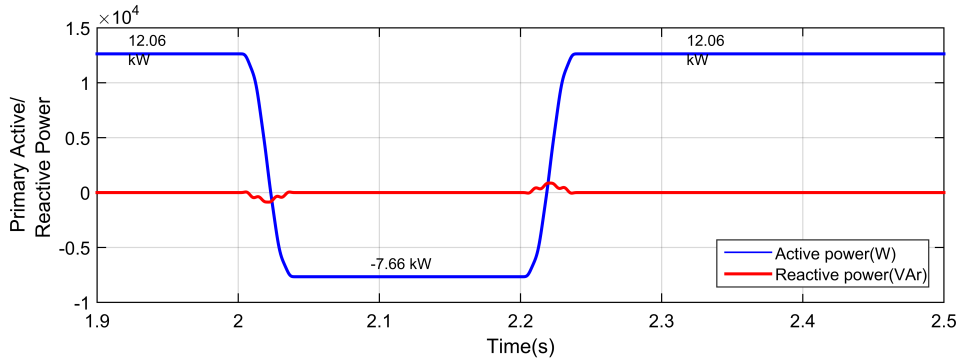

Figure 2.13. Primary side active and reactive power flows under bidirectional mode of operation.

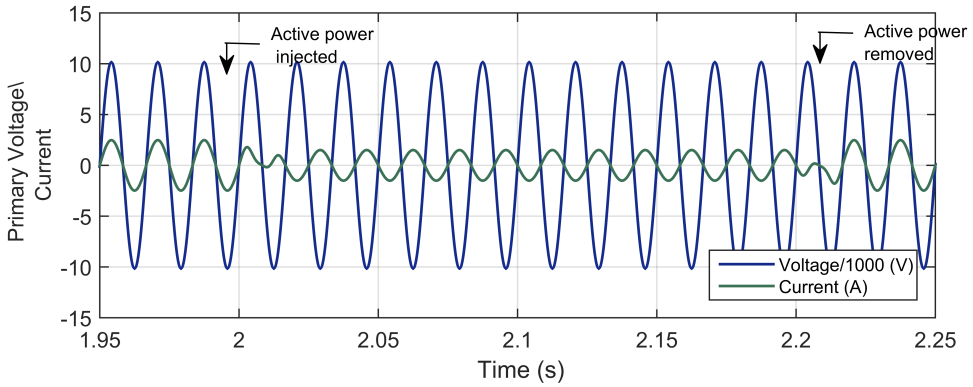

Figure 2.14. Primary side voltage/current waveforms of the solid state transformer bidirectional mode of operation.

2.6.3 Reactive Power Control Function

Another important function of an SST for the purpose of voltage regulation studies in the distribution system is its reactive power compensation capabilities. The developed equivalent model of the SST has the capability to provide the demanded reactive power on the primary side, as illustrated in Fig. 2.15. In this case, a reactive command of 5 kVAr was given to the SST for a simulation time between 0.4 s to 0.6 s. The SST was able to provide the demanded reactive power. The primary side voltage and current waveforms, as shown in Fig. 2.16, was in phase until reactive power was demanded at 0.4 s. From 0.4 s to 0.6 s the current waveform leads the voltage waveform indicating reactive power flow on the primary side of the SST as displayed in the enlarged view of the primary side voltage and current,as shown in Fig. 2.17. But, the designed model achieves this without the use of any complicated control loops.

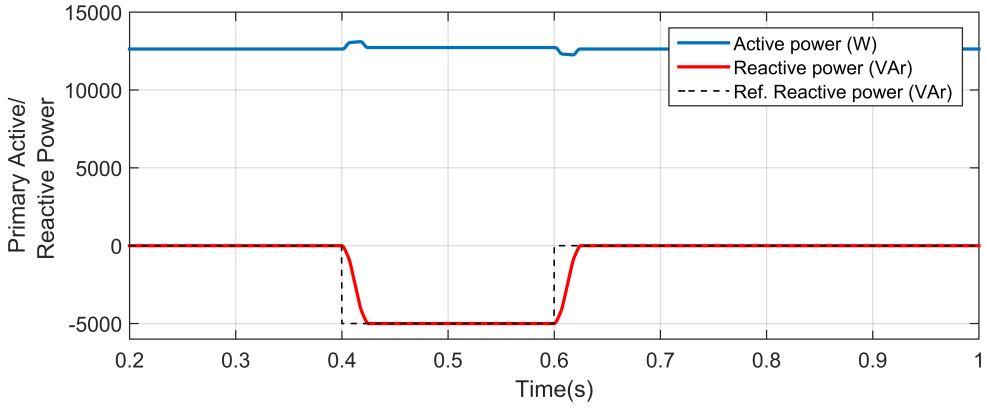

Figure 2.15. Reactive power supplied to the grid by solid state transformer under a given reactive power command.

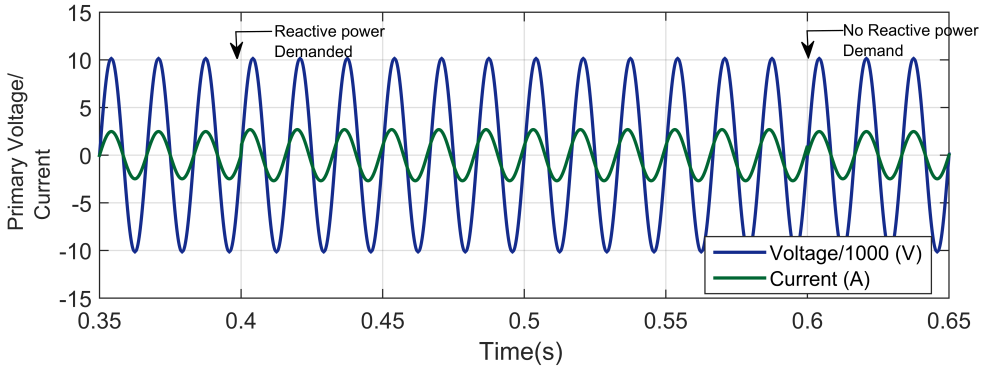

Figure 2.16. Primary side voltage/current waveforms of the solid state transformer under a given reactive power command.

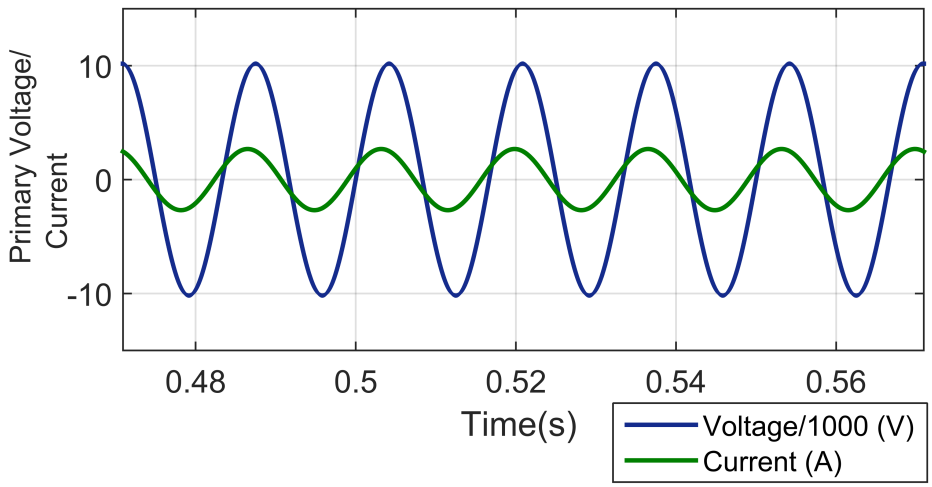

Figure 2.17. Enlarged view of primary side voltage/current waveforms of the solid state transformer under a given reactive power command.

2.7 Summary

A steady-state equivalent model was developed and verified against an average model presented by Zhao et al. [16]. The designed model was tested under load change condition, bidirectional power flow condition and reactive power compensation capabilities as in the average model of SST [16]. The steady-state values of the various parameters were comparable under the same tests that were performed with the average model of SST [16]. Modeling of the losses in the designed SST will need further improvement in the future. The model did have some expected limitations as the switching dynamics of the SST were not captured. However, the main purpose of designing this model was to emulate the behavior of an SST in steady-state with some simple equations without losing its basic functionalities. Based on the simulation results presented, the designed SST model is appropriate for such applications. Moreover, the designed model uses only a few simple equations, the simulations can be performed in

real-time, indicating that the models are suitable for long-term voltage regulation studies. Further, the model can be improved for integration in the distribution systems for voltage regulation by reactive power compensation method.

CHAPTER 3 ACTIVE POWER CURTAILMENT USING ADAPTIVE DROOPS FOR OVERVOLTAGE PREVENTION

3.1 Introduction

The rapid increase in energy demand and environmental concerns due to the excessive consumption of fossil fuels have encouraged the use of RESs. The integration of RESs has extended the capability of the grid as there are different sources to fulfill the load demand. The benefits of RES integration include reducing the cost of energy production, increase in generation capacity, loss reduction, improved voltage profile across the feeder, etc [23]. Recently, the cost reduction in residential PV system has increased the integration of rooftop PV system with the LV distribution systems. However, the intermittent nature of PV generation causes various challenges in LV distribution networks [6].

One of the many challenges that arise during high PV penetration and low loading conditions, is the reverse power flow in LV distribution networks, which increases the voltage at the POC of PV integration [24]. This leads to problems related to power quality and reliability of the system and consequently limits the capacity of PV installation. The power quality problems due to the integration of DG like PV and the wind are sustained power interruptions, voltage regulation, harmonics and voltage sags [25]. Among these problems, this work focuses on voltage regulation. Voltage regulation describes the ability of the system to maintain constant voltage under different load conditions. Voltage should be maintained between certain limits.

There are voltage standards that specify the nominal values of operating voltages for

utilities to maintain the power quality and reliability of electric power systems. According to American National Standards Institute (ANSI) C84.1-2011 [26], voltage standards for service voltage limits are sub-categorized as Range A and Range B. For 240 V nominal voltage systems, Range A limits from 0.95 p.u. to 1.05 p.u. of nominal voltage and Range B limits from 0.917 p.u. to 1.058 p.u. of nominal voltage, as shown in Fig. 3.1. However, the voltage in Range B should be limited for short duration and frequency, and corrective actions are required to limit the voltage within Range A. Thus, the LV distribution network beyond Range B is subjected to overvoltage conditions. The voltage limits established for distributed generation protection ranges from 0.88 p.u. to 1.01 p.u. of nominal voltage. Though the LV distribution network voltage exceeds the Range B, DG protection is not enabled, so the LV distribution network may be subjected to overvoltage conditions in such situations.

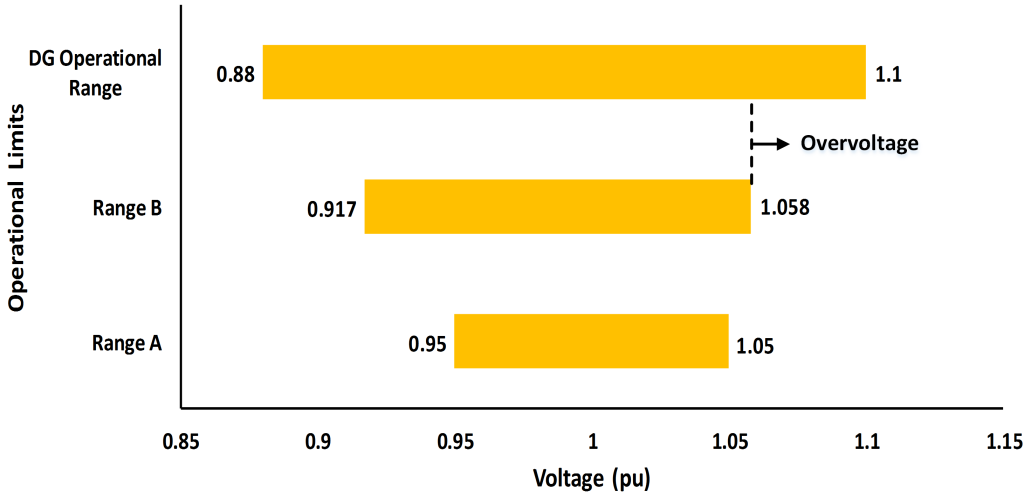

Figure 3.1. Operational limits for 120/240 low voltage distribution networks based on ANSI C84.1-2011 [26] voltage standard and distributed generation (DG) operational voltage limits.

Overvoltage in the system causes high power consumption by the load, the reduction

in the lifetime of the battery, increase in losses in the transformer, and high power dissipation in induction machines [27]. DG like PV and wind have a high generation of active generation at certain times due to its uncertain nature. During such conditions, if the load required in the system is very low, the excess active power causes voltage variations in LV distribution networks as the resistance to reactance (R/X) ratio in LV distribution networks is relatively large. This condition results in overvoltage in the feeder caused by the non-dispatchable PV power. Thus, the proper control method is necessary to eliminate overvoltage in the LV distribution networks integrated with PV systems.

3.2 Previous Work

There are a number of ways to deal with the overvoltage problem as stated in literature such as increasing the conductor size of the overall distribution network, adjusting the taps of LV transformers, using voltage regulators, integrating energy storage systems (ESSs) like batteries, and using APC and reactive power compensation from PV systems [28]. High investment is required in upgrading the conductor size of the overall distribution network. The tap changing option in transformers seems to be a good option but frequent changes in tap settings increases voltage fluctuations. An electronic tap changer using silicon controlled rectifiers were incorporated into primary distribution transformer [29]. However, problems such as transient circulating current between taps and current commutation between the silicon controlled rectifier switches due to winding impedances exist, which increase the system losses. Wu et al. [30] proposed a hierarchical control scheme using distributed ESSs and PV systems for islanded AC microgrids, but incorporating ESSs in LV distribution networks is expensive. The injection of the reactive

power by PV inverters will decrease the voltage rise, but increases losses in the system due to the reactive current flowing in the feeder lines [31]. Moreover, the real power generation and power rating of PV inverter restrict the reactive power capability of a PV inverter. Generally, oversizing of the PV inverters is proposed to extend the reactive power capability of the inverter [28]. Many research works have merged the reactive power compensation methods with other techniques for overvoltage prevention. Olivier et al. proposed [32] a distributed scheme that maintains the active and reactive power output from the PV inverters to prevent overvoltage. The proposed scheme makes use of communication between the controllers among the PV inverters in distributed networks. Similarly, Ghosh et al. [33] proposed a local voltage control using droop-based reactive power injection enhanced by APC. The technique discussed is aided with the tap-changing of voltage regulators and is not self-sufficient.

A droop-based APC method has been discussed for voltage rise mitigation during high PV penetration [8]. Similarly, Chalise et al. [34] implemented APC method for small-scale wind turbines using pitch control to prevent voltage rise. In this literature, a constant value of a droop coefficient is calculated for the worst case scenarios to ensure the voltage is within the pre-defined limits. This results in constrained curtailment that will limit the active power injection by DG in unnecessary conditions. On a similar note, Wang et al. [35] proposed an active power control strategy with an active power limit prediction for continuous update of the droop value. Likewise, Alyami et al. [36] proposed a real power curtailment method that updates the curtailment adaptively to maintain the voltage limit while maximizing PV generation with the objective of fair sharing of the power curtailment. There has been not much research on other types of droop functions other

than constant and linear droop models. Hence, there is a need of exploring other droop models that could maintain the voltage limits with minimum energy loss in the system.

There is a need for a technique that can adjust the droop gains online while reducing the overall power curtailment in the LV network to minimize APC. Conventional droop techniques have restrained droop values that do not change in accordance with PV irradiance and loading conditions. The adjustments in droop have to be such that it does not affect the system stability. A method to adapt the droop gains online using a machine learning based approach known as supplementary adaptive dynamic programming (ADP) controller is proposed in this thesis. Unlike other approaches where the entire droop value is changed, the ADP will be used to generate a supplementary signal that makes slight adjustments to the main droop value like in techniques proposed by Wang et al. [35] and Alyami et al. [36]. The small change in droop value will ensure that the system remains relatively stable as the system does not deviate from its normal operation. The ADP control structure aids in achieving a robust and optimal control simultaneously by solving the Hamilton-Jacobi- Bellman equations of optimal control iteratively through the concept of reinforcement learning [37]. Such approaches have been previously used to solve a number of power system problems [38]–[43].

3.3 Objective

There are two main objectives of this chapter. The first objective is to implement different droop functions in APC method in an LV distribution network with PV systems to study the effect of droop change. The other is to implement the APC method with ADP as a supplementary controller for overvoltage prevention with reduced energy loss in the

LV distribution network.

3.4 Active Power Curtailment Method

Among various methods mentioned in the literature, the APC method stands out to be a good option for LV distribution networks. The reactive power required to keep the voltage across the LV network constant for certain change in the active power can be calculated using Eq. (3.1) [8].

$$Q = -\Delta P \frac{R}{X} \tag{3.1}$$

where Q is the reactive power at the LV distribution network required to keep the voltage constant, ΔP is a change in the active power, and R and X are the resistance and impedance of LV distribution network. Since R/X value for LV distribution network is high, the voltage regulation requires the large value of reactive power. In addition to this, the reactive power injection from the PV inverter is limited during high PV penetration that makes the reactive power compensation unfeasible for the overvoltage prevention. High reactive power leads to the higher circulating current in the network, which causes increased losses. Hence, the overvoltage prevention using the active power would be more effective in the LV distribution networks than the reactive power compensation [44].

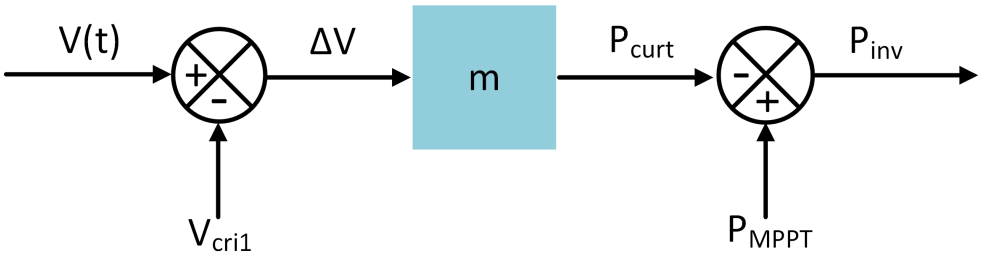

Figure 3.2. Droop-based active power curtailment method for LV distribution networks with PV systems.

Droop-based algorithms are the most popular to coordinate power curtailments in PV inverters for the overvoltage prevention that removes the need for any communication links between those PV inverters [8]. Fig. 3.2 shows the control logic used in droop-based controller. The power injected by the PV inverter (P_{inv}) into the LV network using the droop-based technique can be defined as

$$P_{inv} = P_{MPPT} - m(V(t) - V_{cri}) \tag{3.2}$$

where P_{MPPT} is the maximum power output from the PV system for a given solar irradiance in kW, m is the droop coefficient in kW/V, $V(t)$ is the voltage at the POC of PV system with LV distribution network at particular instant of time t and V_{cri} is the critical voltage above which the power is curtailed to regulate the voltage. When the voltage at the POC $V(t)$ is under normal operating conditions (Range A), i.e., $V(t) < V_{cri}$, then all the power generated from PV system is injected into the LV distribution network, i.e., $P_{inv} = P_{MPPT}$. When $V(t)$ crosses normal operating conditions, i.e., $V(t) > V_{cri}$, then the power is curtailed by a factor of droop coefficient using Eq. (3.2). Thus, the power curtailed ($P_{curtailment}$) during this condition can be shown as in Fig. 3.3 and is given by Eq. (3.3).

$$P_{curtailment} = P_{MPPT} - P_{inv} \tag{3.3}$$

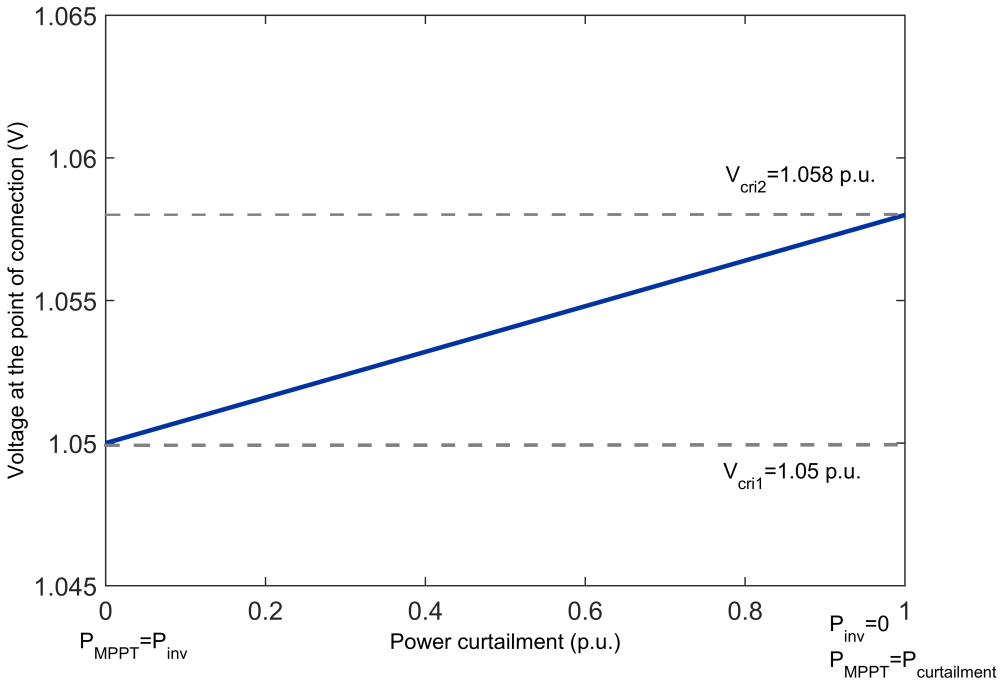

Figure 3.3. Power curtailment in active power curtailment method.

Therefore, this method only operates when the voltage exceeds 1.05 p.u. in the network, allowing maximum power generation in other conditions. APC method curtails the active power if necessary, resulting in lower energy losses in the network due to power curtailment.

3.5 Different Droop Models in Active Power Curtailment Method

3.5.1 System Benchmark

The implementation of different droop models in the APC technique for the overvoltage prevention is highlighted in this section with an example of a typical network model of a residential suburban LV distribution network. The benchmark is taken from the network model of a residential LV distribution network presented by Tonkoski et al. [8], as shown in Fig. 3.4. The LV distribution network consists of twelve houses with each house

having PV system installed. The LV distribution network is connected to the grid by a single phase 75 kVA, 14.4/0.24 kV distribution transformer with split phase supply at the secondary side. The network has a 100 m long feeder line with each house connected by a 20 m long feeder line. Each house is capable of generating 5 kW_p of electrical energy from PV and the annual electricity generation from these houses is about 14,892 kWh. The PV inverter and the house load models are both modeled as voltage dependent current source to depict the instantaneous power flow from and to the houses and PVs. Tables 3.1 and 3.2 show the parameters for the LV transformer and network line parameters for the single phase PI section line, respectively.

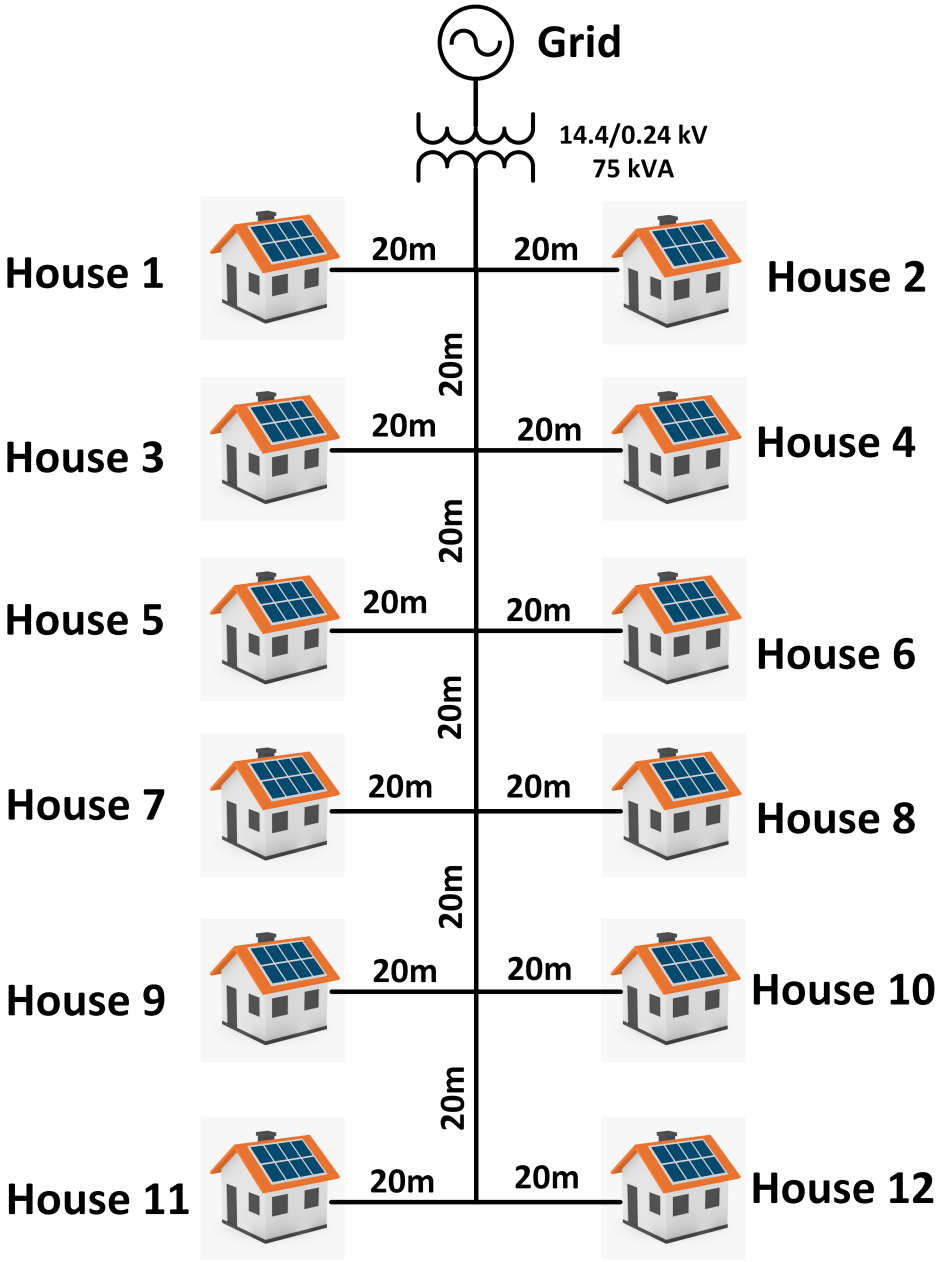

Figure 3.4. A rural low voltage distribution network.

Table 3.1. Single phase Low voltage transformer parameters

Transformer parameters	**Value**
Primary winding resistance	0.006 p.u.
Primary winding leakage inductance	0.020 p.u.
Secondary winding resistance	0.012 p.u.
Secondary winding leakage inductane	0.025 p.u.
Magnetizing resistance	500 p.u.
Magnetizing inductance	500 p.u.

Table 3.2. Single phase PI section line parameters

Line Parameters	**Drop Lines**	**Pole-Pole Lines**
Resistance (Ω/km)	0.549	0.346
Inductance (mH/km)	0.23	0.24
Capacitance (μF/km)	0.055	0.075

APC was implemented in the system benchmark using different droop models, categorized as linear, quadratic, and exponential. The simulation model was built in MATLAB/Simulink with solar irradiance and load profile as inputs for the benchmark. The simulation model was run with the solar irradiance data and load profiles for a day, as shown in Fig. 3.5. The solar irradiance data was taken from SAMS software for Minneapolis, Minnesota for a sunny day [45]. The PV size was 5 kWp for all the twelve houses. The load profile was estimated using Poisson process and Queue theory for a day [45], [46]. These techniques modeled energy consumption profile for each household appliances based on their consumption pattern and later summed up to get the load profiles of the houses. To generalize the different load profiles of the twelve houses, the average load is plotted in Fig. 3.5. The resolution of one hour was taken for the solar irradiance data and load profiles, which is good enough to approximate steady state conditions. The profiles shows that high PV generation and low loading condition occurs at 1 pm in the modeled case.

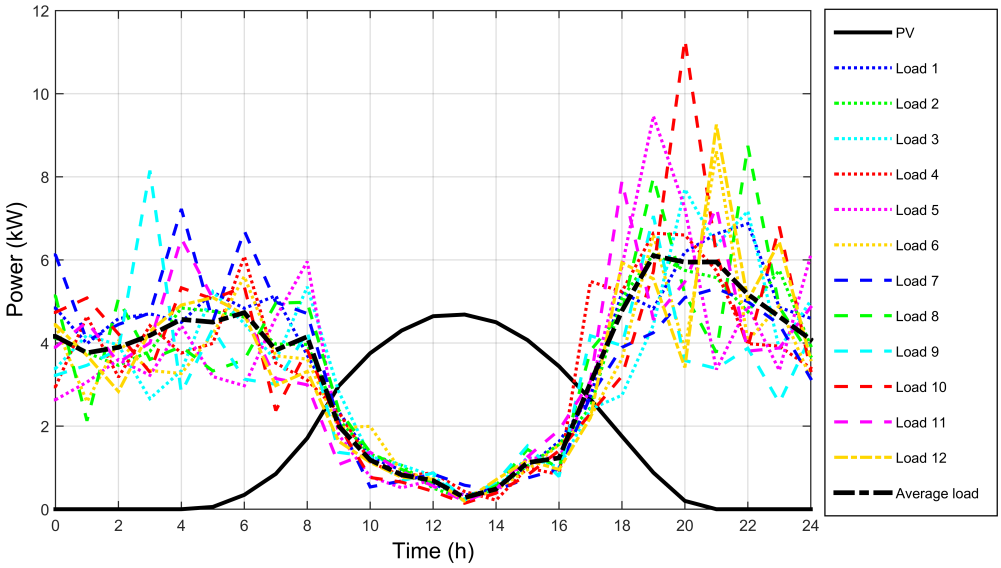

Figure 3.5. Solar PV power and house load profile (House 1 to House 12) for a day.

This section presents the simulation results for the twelve-house model with four simulation cases: a base case without overvoltage prevention and droop-based APC method with linear, quadratic, and exponential droop models. The simulation was performed without any droop control for the base case and the droop-based APC method was implemented for the latter cases. All the cases were simulated with same PV power data and corresponding load profile for each house.

3.5.2 Base Case

Base case represents the method in which the PV inverters inject full MPPT power until the voltage at POC reaches 1.1 p.u., and then the system shuts down after the voltage exceeds 1.1 p.u. This is the simplest case for the system benchmark to compare the effectiveness of the APC method.

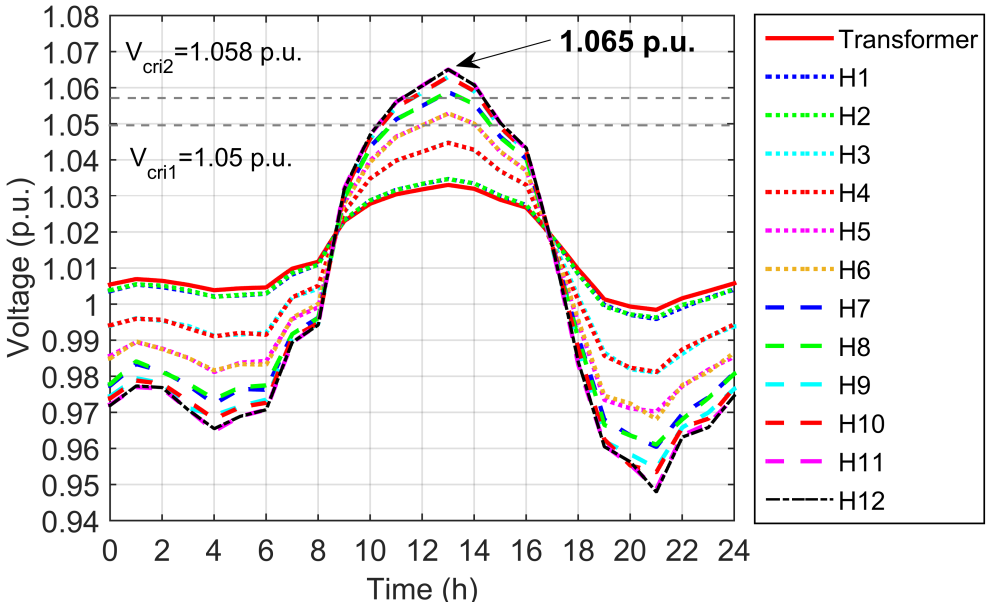

Figure 3.6. Voltage profile of twelve houses (House 1 to House 12) in the base case.

Fig. 3.6 shows the voltage profile in the base case, without any droop-based APC overvoltage prevention method. The voltage profile for houses at the same POC of the LV distribution network, are same and equal in values. The maximum voltage of 1.065 p.u. occurred at 1 pm in houses 11 and 12, that was above V_{cri2} in the base case simulation. Similarly, houses 7 to 12 undergo overvoltages, that is, the voltage exceeds V_{cri2} (1.058 p.u.), during the 24 hour simulation time period in the base case simulation. The energy output from PV for each case was calculated by determining the area under the power curve. The energy output from all the PV inverters summed up to be 489.60 kWh in base case simulation for 24 hour period.

3.5.3 Linear Droop

The second case represents the method in which all the PV inverters have droop-based APC control. All the PV inverters have same droop coefficients which

linearly curtails power, as shown in Fig. 3.7. The droop coefficient is calculated so that the curtailment occurs between critical voltages, i.e., 1.05 p.u. and 1.058 p.u. In this case, the droop coefficient is a constant value and the power curtailment occurs in a linear way with the droop coefficient as the slope of the linear function. The droop coefficient was calculated using Eq. (3.4).

$$m = \frac{P_{max}}{(V_{cri1} - V_{cri2})} = 2.5\frac{kW}{V} \tag{3.4}$$

where P_{max} is the maximum power to be curtailed by PV inverter during the voltage limit from V_{cri1} (1.05 p.u. of 240 V, upper limit of Range A) to V_{cri2} (1.058 p.u. of 240 V, upper limit of Range B).

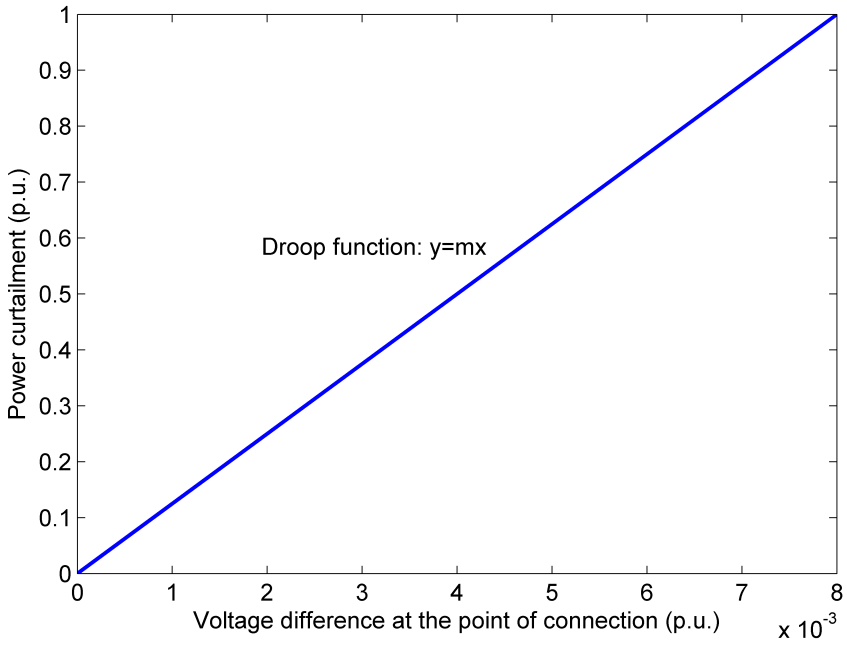

Figure 3.7. Linear droop with constant droop coefficient (m) as slope for active power curtailment method.

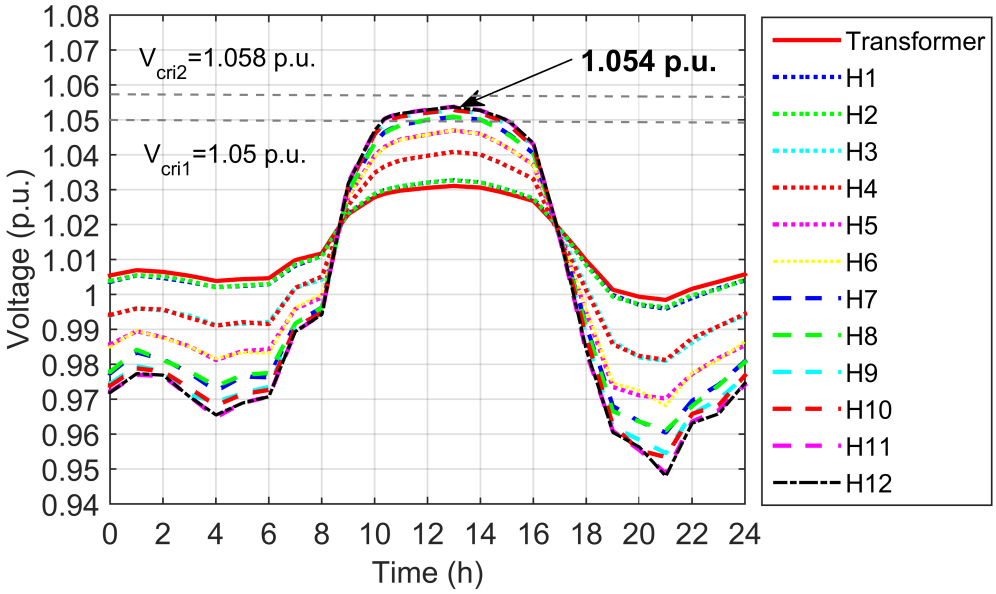

Figure 3.8. Voltage profile of twelve houses (House 1 to House 12) in the droop-based active power curtailment method with linear droop.

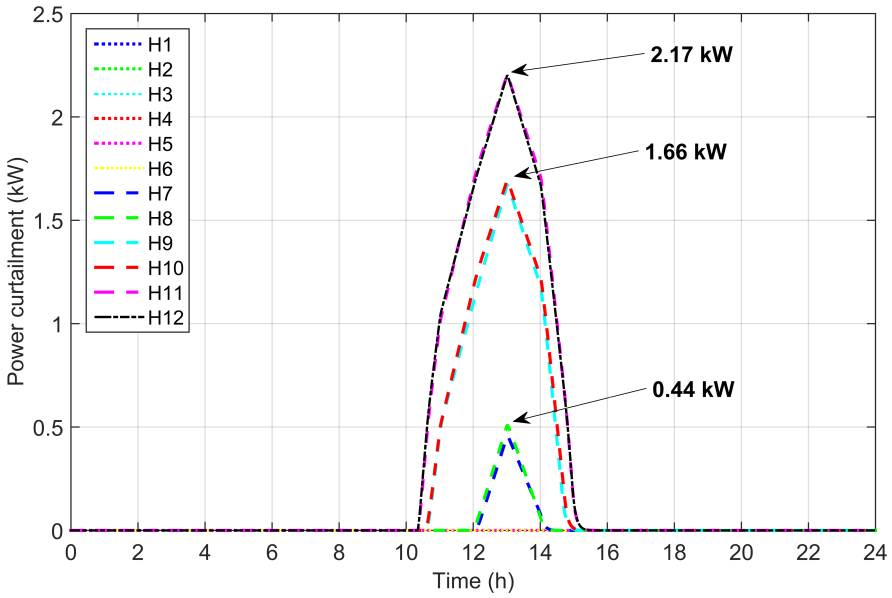

Figure 3.9. Power curtailment in the droop-based active power curtailment method with linear droop.

After the implementation of the droop-based APC method, the maximum voltage at houses 11 and 12, as shown in Fig. 3.8 is 1.054 p.u., which is less than V_{cri2}. Similarly,

none of the houses exceed the voltage above V_{cri2}. Fig. 3.9 shows the power curtailed during APC implementation with linear droop. The maximum power curtailed at 1 pm was 2.17 kW. The energy output from PV decreased from 489.60 kWh in the base case simulation to 466.87 kWh in the simulation with the linear droop-based APC for all the twelve houses. The overall energy loss due to curtailment was 22.72 kWh.

From above results, it can be concluded that the overvoltage condition is resolved, but the power injection from PV is decreased, resulting in energy loss that could be utilized. However, PV systems should be capable of injecting maximum PV power available without being subjected to overvoltage or disconnected due to the violation of protection limits. Therefore, an approach that maximizes the active power injection from PV systems while allowing the voltage under V_{cri2} for short period is the main motivation of this work.

3.5.4 Quadratic Droop

In the third case, the PV inverters are controlled with droop-based APC method, but the droop parameters were guided by a quadratic function as shown in Fig. 3.10. When the voltage at the POC exceeds V_{cri1} (1.05 p.u.), droop-based APC begins to curtail power injected by the PV inverter on the basis of droop function until the voltage reaches V_{cri2} (1.058 p.u.), where maximum curtailment occurs. The same logic can be summarized using values in per unit form. When the voltage difference at the POC (ΔV) is 0, there is no power curtailment. Similarly, when the voltage difference at the POC (ΔV) is 0.008 p.u., the power curtailment is 1 p.u. The quadratic function was determined from these points using the curve fitting tool in MATLAB. The quadratic droop function obtained is

given by Eq. (3.5).

$$y = 1.52 \times 10^4 x^2 \tag{3.5}$$

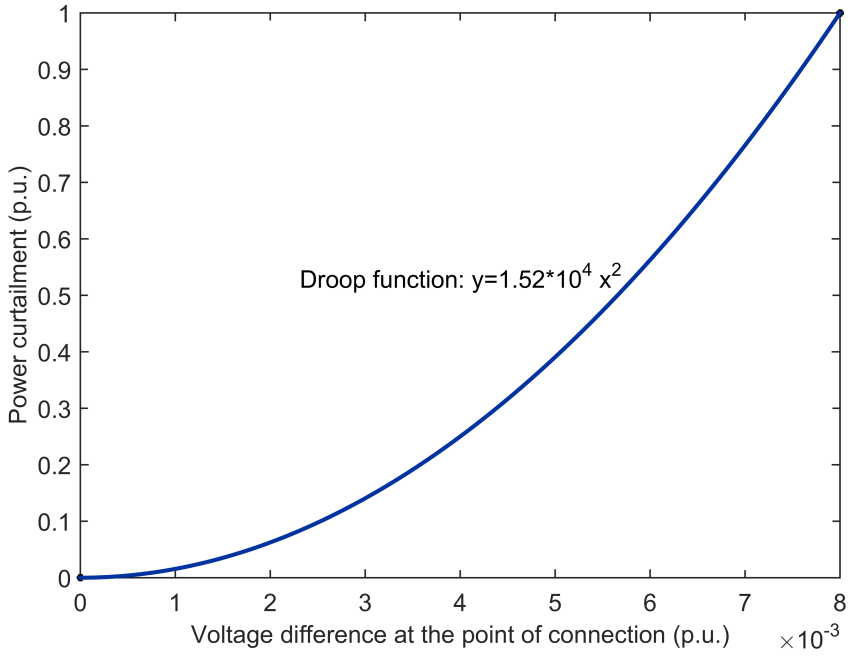

Figure 3.10. Quadratic droop function for active power curtailment method.

Fig. 3.11 shows the voltage profile of the twelve houses with the droop-based APC method with a quadratic function. The maximum voltage of 1.056 p.u. occurs at 1 pm in houses 11 and 12, which does not exceed the critical value V_{cri2} (1.058 p.u.). The maximum voltages in houses from 7 to 12 are higher in APC method with quadratic function than in APC method with linear droop. Likewise, APC method with constant droop, the voltages for all the houses in APC with quadratic droop are below V_{cri2}.

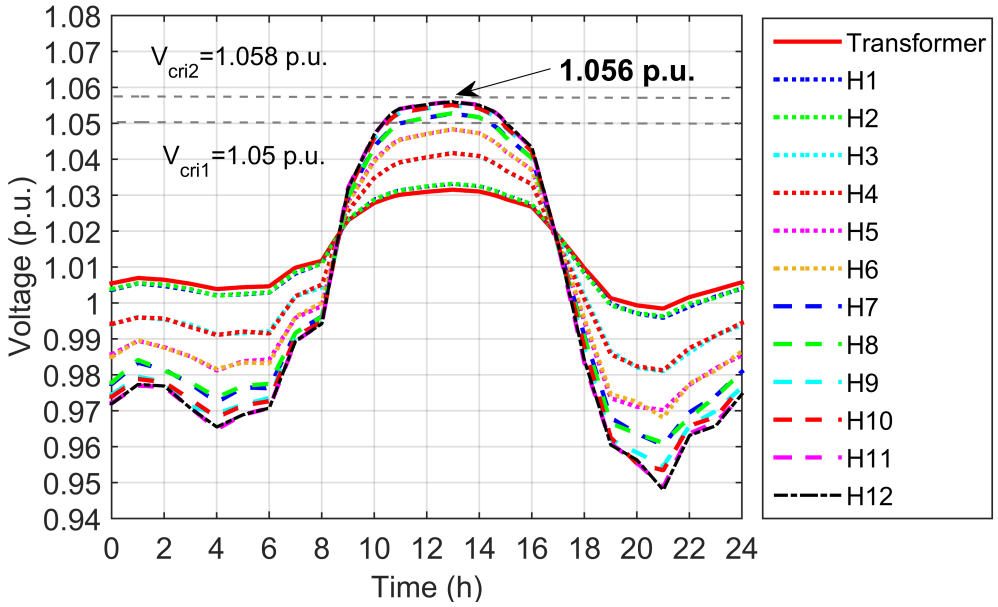

Figure 3.11. Voltage profile of twelve houses (House 1 to House 12) in the droop-based active power curtailment method with quadratic droop.

Fig. 3.12 presents the power curtailed during the implementation of the quadratic droop-based APC method. The maximum power curtailment is 1.98 kW at houses 11 and 12, which is less than that in constant droop-based APC method. The power curtailments for houses 7 to 12 are less than that of APC method with linear droop. In the same way, the energy output from the PV inverters of the twelve houses is 474.32 kWh, which is greater than of APC method with linear droop. The energy loss due to curtailment is 15.27 kWh.

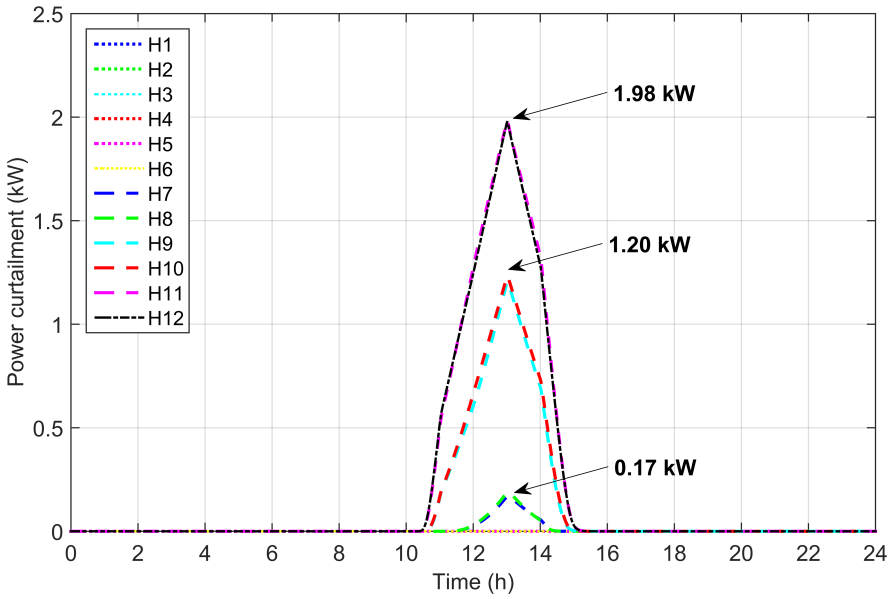

Figure 3.12. Power curtailment in the droop-based active power curtailment method with quadratic droop.

3.5.5 Exponential Droop

Similar to the quadratic droop case, this case has droop-based controllers in PV inverters driven by an exponential droop function. The exponential function is determined by using the values of voltage difference at the POC (ΔV) and power curtailment in per unit as explained in quadratic droop and the fitted equation is achieved, as shown in Fig. 3.13. The exponential droop function obtained is given by Eq. (3.6).

$$y = 0.00516e^{650x} \tag{3.6}$$

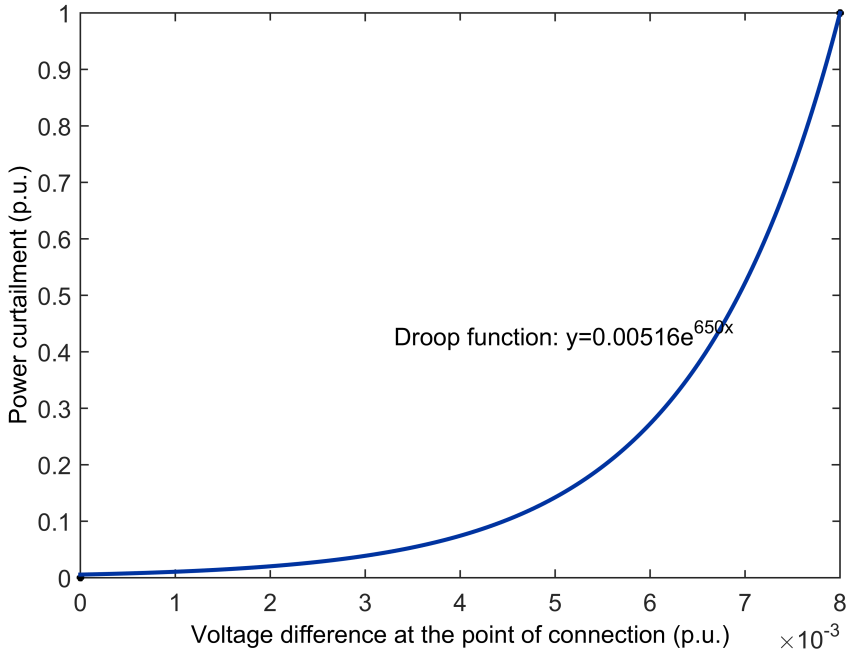

Figure 3.13. Exponential droop function for active power curtailment method.

Fig. 3.14 presents the voltage profile of the twelve houses after using APC method using the exponential function. The maximum voltage at houses 9 to 12 is 1.057 p.u., which is less than V_{cri2}. House 9 to 12 do not experience overvoltage at any time of the 24 hour period.

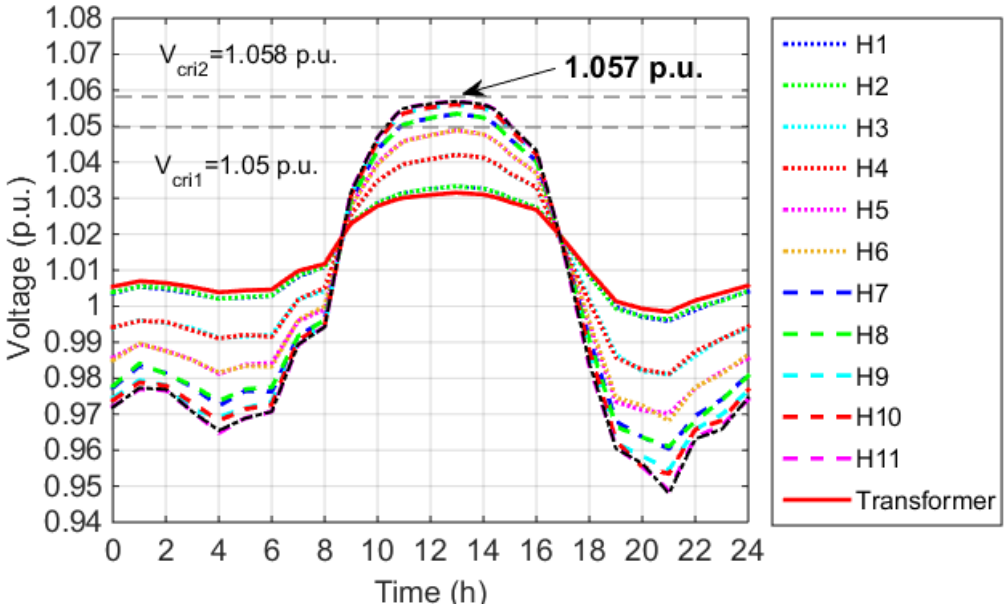

Figure 3.14. Voltage profile of twelve houses (House 1 to House 12) in the droop-based active ower curtailment method with exponential droop.

Fig. 3.15 shows the power curtailment by the houses in APC method using exponential droop. The maximum power curtailment is 1.92 kW for houses 11 and 12, which is slightly less than that in APC method with quadratic droop. The curtailments from house 7 to 12 are the lowest in this method compared to above droop-based APC techniques. The energy output from the houses is 477.20 kWh, which is maximum among droop-based APC methods. Thus, the energy loss in APC method with exponential droop is 12.40 kWh.

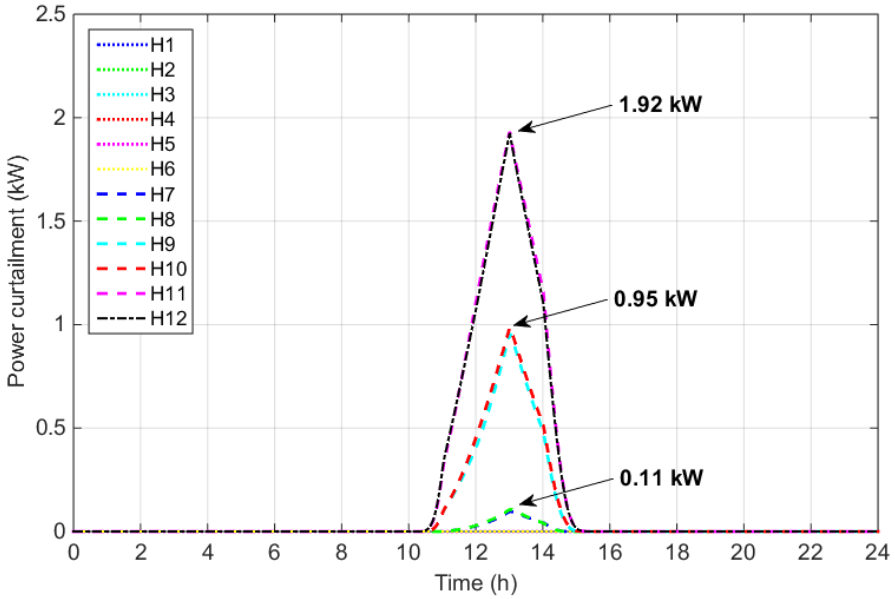

Figure 3.15. Power curtailment in the droop-based active power curtailment method with exponential droop.

In summary, changing droop function from the fixed value maintains the voltage profile of the farthest houses at the upper boundary of the operating condition. The power curtailment for overvoltage prevention decreases in such techniques while maintaining the voltage within acceptable limits. Fig. 3.16 presents the energy output from the PV inverters and the energy losses due to curtailment in the APC method with different droop functions. The energy output from the PV inverters increases and energy losses due to curtailment decrease as the fixed droop are changed to quadratic or exponential function. The energy losses due to curtailment in each house and its overall sum are listed in Table 3.3. The energy losses in each house decrease in both quadratic and exponential droops resulting in reduced overall energy loss than in linear droop. This points out that changing the droop coefficient can reduce unnecessary power curtailments in PV inverters in APC technique. However, the droop value is based on a particular function that does

not adapt itself to reduce the curtailment. A flexible method is required that can update the droop value accordingly in the system for minimum curtailment. Also, stability analysis of the APC method with quadratic and exponential droops is necessary for validating the possibility of such techniques in the real scenario.

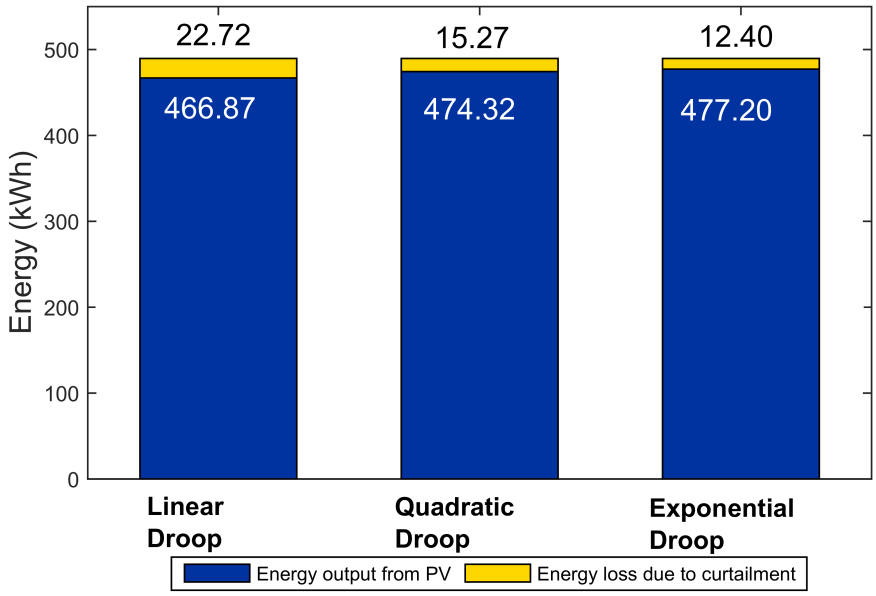

Figure 3.16. Energy output from PV and energy loss in different droop models .

Table 3.3. Energy losses in twelve houses due to curtailment using different droop models

Houses	**APC-Linear Droop (kWh)**	**APC-Quadratic Droop (kWh)**	**APC-Exponential Droop (kWh)**
H1	0	0	0
H2	0	0	0
H3	0	0	0
H4	0	0	0
H5	0	0	0
H6	0	0	0
H7	0.48	0.22	0.15
H8	0.54	0.23	0.16
H9	4.18	2.49	1.79
H10	4.36	2.63	1.90
H11	6.59	4.87	4.24
H12	6.56	4.81	4.16
Total	**22.72**	**15.27**	**12.40**

3.6 Adaptive Droop using Adaptive Dynamic Programming

3.6.1 Droop Adjustment Based on Adaptive Dynamic Programming

The droop-based control technique curtails the power on the basis of fixed factor for all the cases, which results in an unnecessary decrease of PV power generation [35]. As shown in Fig. 3.8, there is a voltage band that exists between Range A and Range B. The voltage can cross Range A for certain duration before it reaches the overvoltage criteria. Increasing the power injection by PV inverters to the extent that the voltage can be restricted to the boundary condition of overvoltage is a good option. This can reduce the curtailment and at the same time will keep the voltage under the operational limits. Thus, a control strategy that can constantly update the droop coefficient is required, such that the power curtailment can be minimized along with the overvoltage prevention.

In this work, ADP is proposed as a supplementary controller to set the droop coefficient in an adaptive way for the overvoltage prevention. The voltage difference and the power curtailment are the input signals to ADP controller such that the information on both the objectives, i.e., the overvoltage prevention and the power curtailment minimization, has been provided [41]. ADP is a machine learning based approach to optimize the performance of dynamic systems over time. ADP controller consists of two neural network structures, as shown in Fig. 3.17. The structure consists of an action network, which is responsible for generating the control action while the critic network, based on a "reward" signal, optimizes the weights of the action network. The action network is a 6-6-1 structure with inputs $X_1, X_2, X_3, X_4, X_5,$, and X_6. X_1 is the per unit value of the difference between $V(t)$ and V_{cri1}. X_2 and X_3 are the per unit values of the one-time

step and two-time stepped delayed values of the voltage difference, respectively. Similarly, X_4 is the per unit value of the power curtailment. X_5 and X_6 are the per unit values of the one-time step and two-time stepped delayed values of the power curtailment, respectively. There are six hidden nodes H_1 to H_6 and an output node u. The output of the action network is the droop coefficient value (m_{ADP}) used for adjustment of constant droop coefficient (m_c) to obtain the total droop coefficient (m_T) for proposed adaptive droop-based APC. The critic network is a 7-6-1 structure with inputs X_1, X_2, X_3, X_4, X_5, X_6, and u. There are six hidden nodes H_1 to H_6 and an output node J.

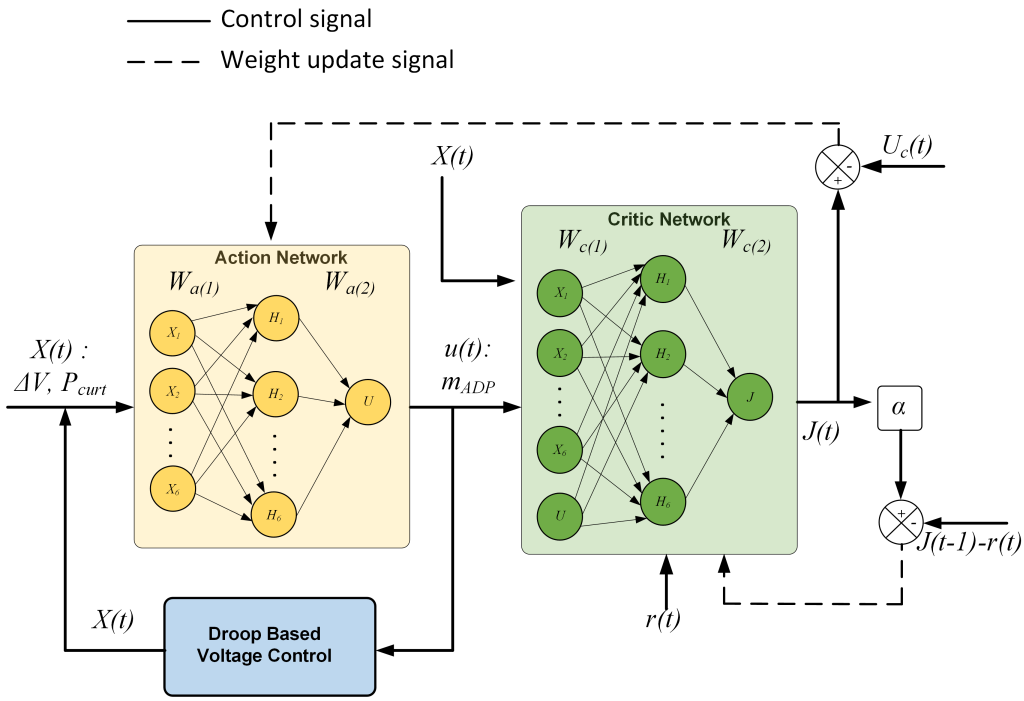

Figure 3.17. Structure of adaptive dynamic programming (ADP) controller with action and critic network.

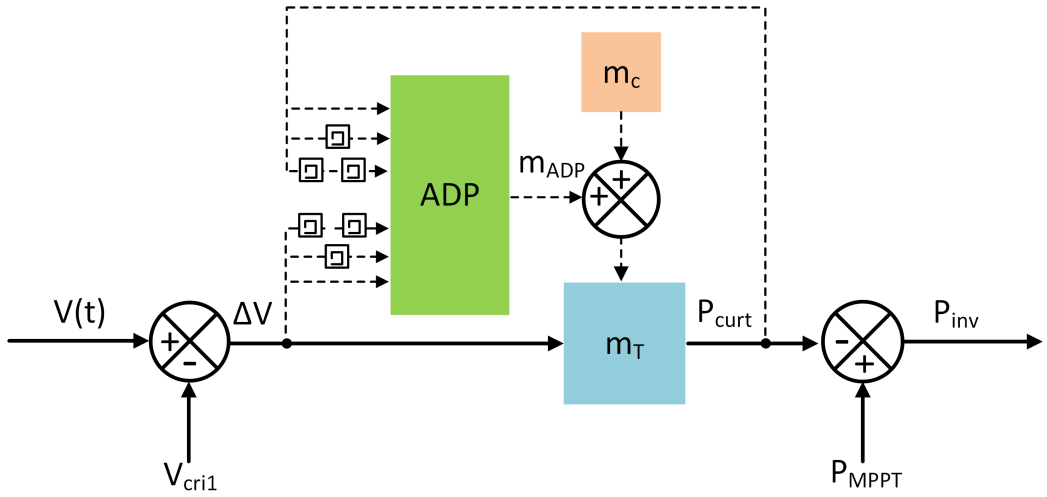

Figure 3.18. Adaptive dynamic programming controller for adaptive droop control with droop-based active power curtailment method.

The critic network in an ADP structure is designed in such a way that the optimal cost function $J^*(X(t))$ satisfies the Bellman principle of optimality such that

$$J^*(X(t)) = \min_{u(t)} \{J^*(X(t+1)) + r(X(t)) - U_c\} \tag{3.7}$$

where, $r(X(t))$ is the immediate cost incurred by $u(t)$ at time t and U_c is a heuristic term used to balance. As shown in Fig. 3.17, the output of critic network updates the weight of the action network, as the value of U_c is set 0 for our design. The reward signal can be defined in a binary format with "0" representing success or "-1" representing a failure. In this paper, the following reward signal will be used,

$$r(t) = -c(a_1 X_1^2 + a_2 X_2^2 + a_3 X_3^2 + a_4 X_4^2 + a_5 X_5^2 + a_6 X_6^2) \tag{3.8}$$

where $c, a_1, a_2, a_3, a_4, a_5$, and a_6 are constants. The reward signal is designed to restrict the

voltage from crossing V_{cri2} with reduced curtailment possible. For designing the reward signal for ADP algorithm, the value of c in above equation was taken as 1, whenever there is a positive voltage difference and power curtailment. The reward signal is generated for adjusting the weights of the action network accordingly. The values for a_1, a_2, a_3, a_4, a_5, and a_6 were taken as 0.1, 0.1, 0.1, 0.4, 0.2, and 0.1 respectively. Fig. 3.18 shows the control logic of the droop-based APC with ADP for adjusting the value of the droop coefficient with an objective of minimizing the power curtailment such that $V(t) < V_{cri2}$ and $0 < P_{inv} \leq P_{MPPT}$.

3.6.2 Simulation Results

The APC method with adaptive droop using ADP was implemented in each PV inverters of the twelve house model. The simulation time step was taken as 100μs, so the time delay for one time and two time-delayed feedback signal of frequency were 100μs and 200μs respectively. The ADP was coded in s-function block of MATLAB/Simulink. The initial weights of the action and the critic network of ADP were randomly initialized between -0.1 and 0.1. The voltage at the POC and power curtailment were given as inputs in per unit form so that it can be used in any network parameters. The neural networks were trained offline with the parameters used by Malla et al. in [39]. The voltage at the POC is same for the symmetrical houses in every 20 m distance of the backbone of the feeder line. An ADP controller for each house pair was used to update the droop of the symmetrical houses during the training of the ADP. The network can be provided with a simple communication link between each house pair for exchanging voltage, power curtailment, and droop coefficient values. The ADP controllers are used in odd numbered

houses and the average value of the voltage at POC and power curtailment of the houses in the house pair are used for training purpose. The adjustment of the droop values is sent to the even numbered houses by its house pair through the same communication link. The training was done until reduced power curtailment was achieved for voltage at POC for all the houses being under allowable limits. The final trained weights were used for testing the technique.

The control algorithm was tested with and without online updating of the critic network. For the first case, the trained weights were directly used in the simulation to obtain the results. For the latter case, the online updating by the critic network was implemented with a very small learning rate. The learning rate used for the testing phase was 0.001. The online learning in ADP updates the action of the control through reinforcement learning to improve the performance of the controller. The output of the critic network, J updated the weights of action network online, which made the system adaptive.

Fig. 3.19 presents the voltage profile of the twelve houses after using APC method using ADP without any online updating by the critic network. The maximum voltage at houses 9 to 12 is 1.057 p.u., which is less than V_{cri2}. The voltage at the farthest houses, i.e., houses 9 to 12 is closer to the upper boundary of the allowable voltage band. Fig. 3.20 shows the power curtailment by the houses in APC method using ADP without any online updating by the critic network. The maximum power curtailment is 1.23 kW for houses 11 and 12, which is lower than that in droop-based APC method by 0.94 kW. The maximum curtailments from houses 7 to 10 are 1.12 kW.

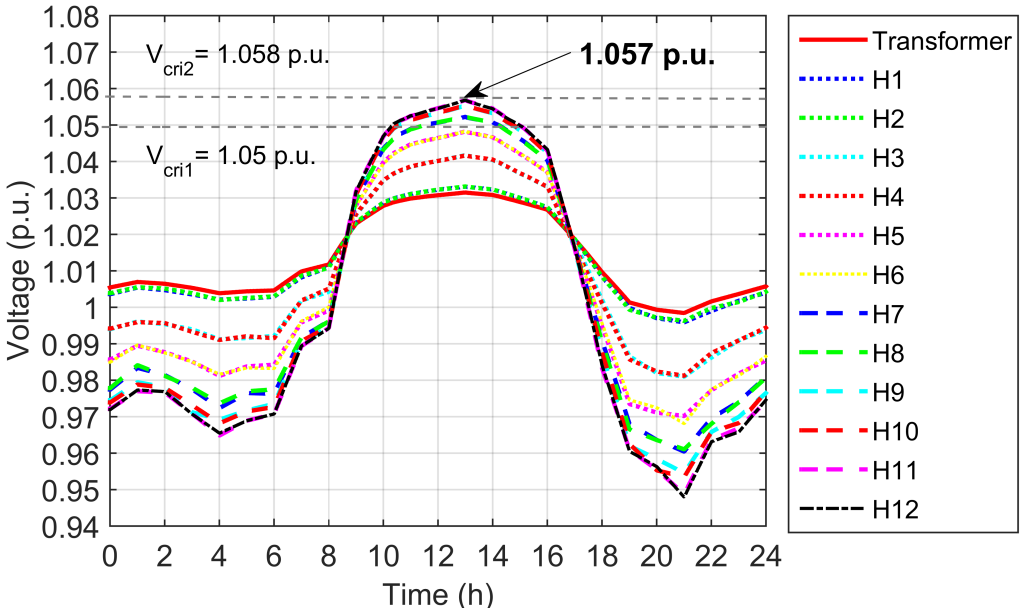

Figure 3.19. Voltage profile of twelve houses (House 1 to House 12) in the droop-based active power curtailment method using adaptive dynamic programming without online updating by the critic network.

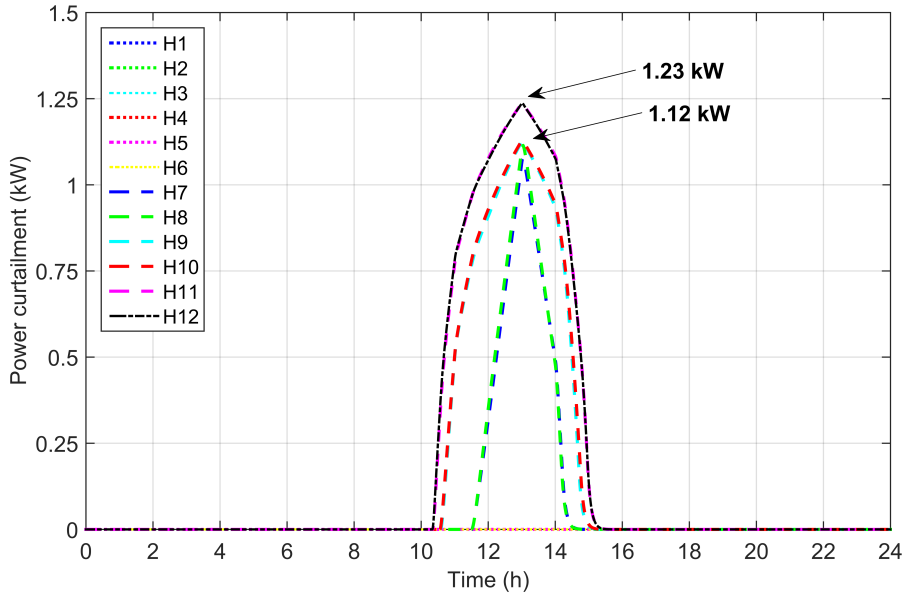

Figure 3.20. Power curtailment in the droop-based active power curtailment method using adaptive dynamic programming without online updating by the critic network.

Fig. 3.21 presents the voltage profile of the twelve houses after using APC method

using ADP with the online updating by the critic network. The maximum voltage at houses 9 to 12 is 1.057 p.u., which is less than V_{cri2}. The voltage profile for the houses is same as in the case with ADP without any online update. Fig. 3.22 shows the power curtailment by the houses in APC method using ADP with the online updating by the critic network. The maximum power curtailment is 1.25 kW for houses 11 and 12. The maximum curtailments from house 7 to 10 are 1.11 kW.

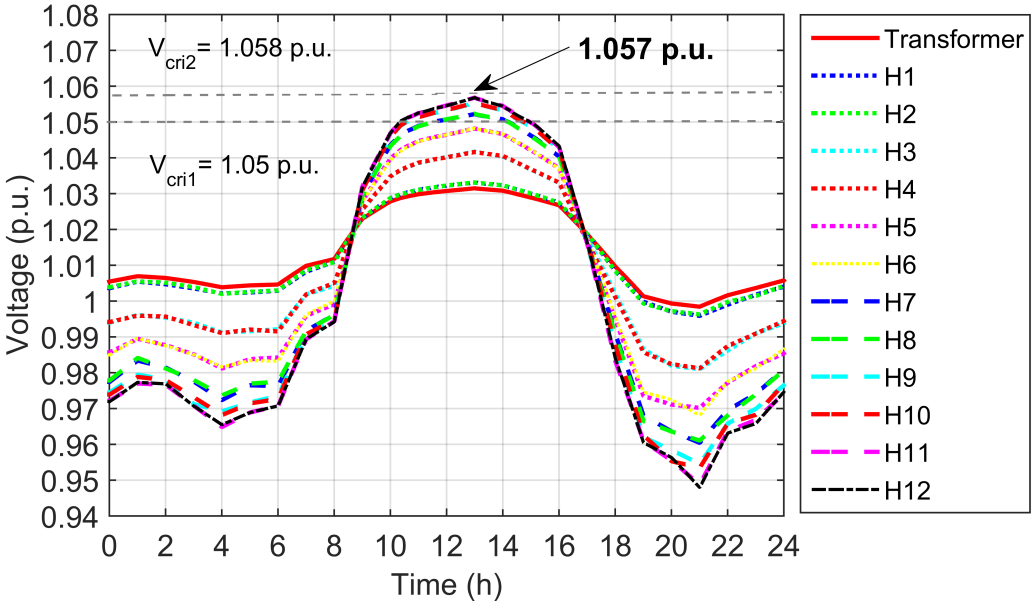

Figure 3.21. Voltage profile of twelve houses (House 1 to House 12) in the droop-based active power curtailment method using adaptive dynamic programming with online updating by the critic network.

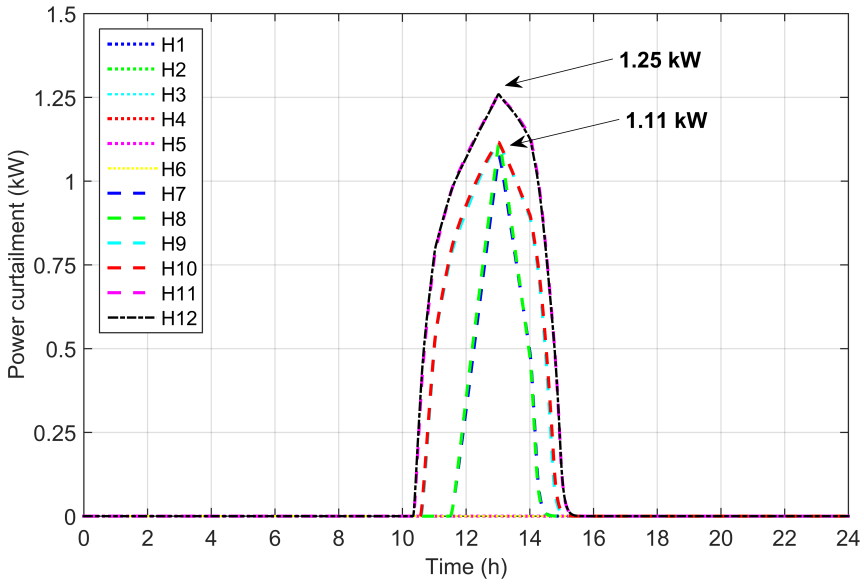

Figure 3.22. Power curtailment in the droop-based active power curtailment method using ADP with online updating by the critic network.

Fig. 3.23 presents the energy output from the PV inverters and the energy losses due to curtailment in the APC method with adaptive droop using ADP. The energy output forms the PV inverters increases and energy losses due to curtailment decreases by using adaptive droop using ADP. The energy losses due to curtailment in each house and the total energy loss of the system are listed in Table 3.4. The energy losses in each house are more distributed in APC with ADP cases than in droop-based APC case. The two cases for APC with ADP also do not show any significant difference. Also, the power curtailment and energy output values have changed slightly, but show the same behavior in both cases, proving that the droop values changed in the system.

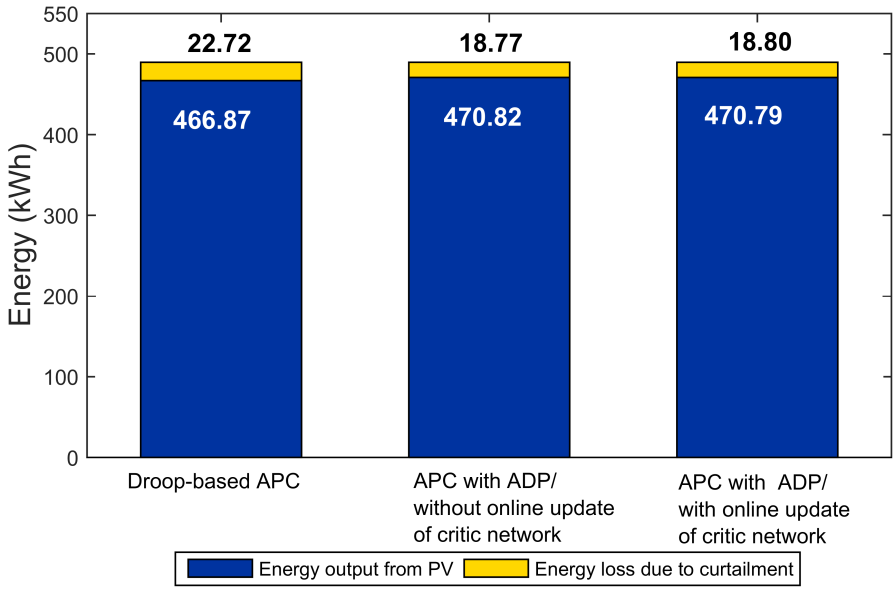

Figure 3.23. Energy output from PV and energy loss in active power curtailment method and active power curtailment method using adaptive dynamic programming with and without online updating by the critic network .

Table 3.4. Energy losses due to curtailment in active power curtailment method and active power curtailment method using adaptive dynamic programming with and without online update by the critic network

Houses	**Linear droop-based APC (kWh)**	**APC using ADP without online update of critic network (kWh)**	**APC using ADP with the online update of critic network (kWh)**
H1	0	0	0
H2	0	0	0
H3	0	0	0
H4	0	0	0
H5	0	0	0
H6	0	0	0
H7	0.48	1.65	1.65
H8	0.54	1.71	1.71
H9	4.18	3.37	3.31
H10	4.36	3.44	3.38
H11	6.59	4.29	4.36
H12	6.56	4.29	4.37
Total	**22.72**	**18.77**	**18.80**

Fig. 3.24 presents the energy losses due to curtailment in the APC method with linear, quadratic, and exponential droops and APC method using ADP. The energy loss in ADP based APC is not the least among the different droop models implemented in APC method. ADP based APC method can be implemented using quadratic and exponential droop for further analysis of the adaptive droop technique in future.

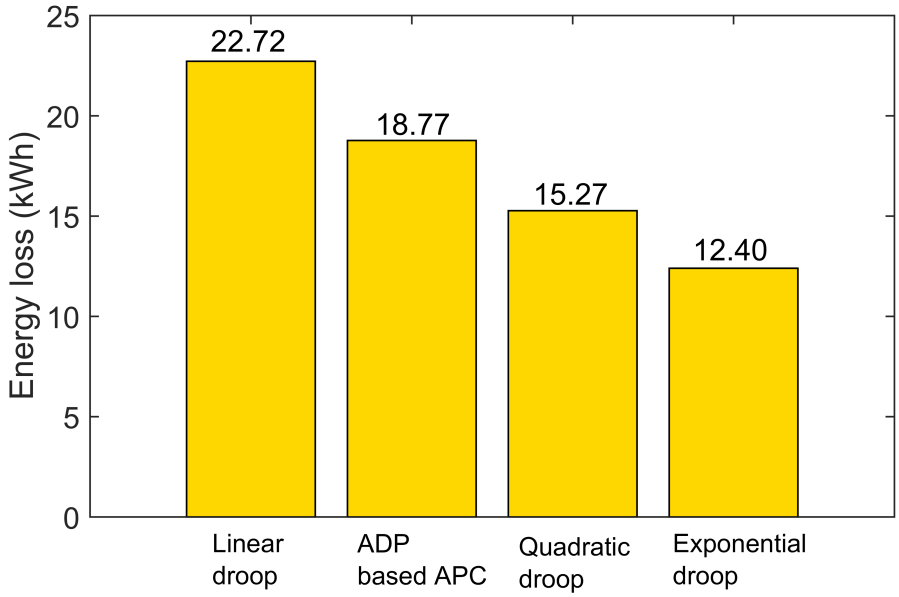

Figure 3.24. Energy loss in active power curtailment method with linear, quadratic, and exponential droops and active power curtailment method using adaptive dynamic programming.

3.7 Summary

APC demonstrates to tackle with overvoltage problem in LV feeders with high DG penetration. The constant droop value in APC method results in constrained curtailment, that restricts power injection by DG in the grid. The APC method was implemented in the system benchmark with different droop models. The constant droop-based APC method resolved the overvoltage problem during high PV penetration and low loading condition. Energy loss in the system occurs due to the curtailment which reduced the PV power

injection in the grid. APC method with quadratic and exponential functions was able to reduce the energy loss in the system while maintaining the voltage profile within acceptable limits. Thus, this demonstrates that changing the droop coefficient can decrease energy loss in individual houses and total energy loss in the overall system. However, the droop values were constrained to a particular function in all the houses.

An adaptive approach to adjust the droop values was proposed using ADP. The adaptive droop-based APC method using ADP was implemented in the system benchmark and its performance was analyzed. The voltage profile of the twelve houses was closer to the upper boundary of the allowable voltage limit. The APC with ADP method reduced the energy loss in the system by 17.4%. Moreover, the energy loss in the houses downstream the feeder was more distributed than in constant droop-based APC method. Therefore, ADP based APC method increased the DG penetration in the feeder by reducing the power capping.

CHAPTER 4 CONCLUSIONS

4.1 Conclusions

Energy demand can be fulfilled by increasing the use of renewable energy resources for energy production with less environmental harm. With increasing integration of DG like PV in the LV distribution networks, voltage regulation has become one of the main challenges that needs to be addressed. Voltage regulation is a very important measure that ensures power quality and reliability of the distribution network. Voltage regulation in both distribution level and at the POC of DG integration in the LV distribution network has been studied widely either separately or in conjunction with the other. The DG systems connected in the LV distribution network can cause the upstream flow of power towards the grid. This results in voltage rise in the system at certain locations than the acceptable voltage limits. Therefore, the integration of DG is limited in the distribution network causing loss of useful energy. For maximizing the integration of DG while maintaining the voltage limits of the system, SST in distribution level is proposed and APC technique with adaptive-droop at the POC is proposed in this thesis.

SST has been recognized as one of the most evolving technologies in the field of the distribution system with the improvement in wide band-gap semiconductors. The reactive power compensation capability of the SST can be used for voltage regulation at the distribution level in the LV distribution network. The controllable power electronic converters and reactive power compensation are the most important characteristics of SST that can be utilized in voltage regulation. The current models of SST are complex for use in large systems for voltage regulation studies. A fairly simple model that captures the

basic functionalities of SST like bidirectional power flow and reactive power compensation capabilities in steady-state, is required for large and complex simulations of distribution network models. Hence, a steady-state equivalent model of SST was developed and verified against an average model. The developed SST can be used for real-time simulations of long-term voltage regulation studies.

APC method prevents overvoltage at the point of connection of DG in LV distribution network. Power curtailment increases at the PV inverters that are farther from the LV transformer in the distribution network. Fixed droop in APC method causes unnecessary curtailment even though the voltage is maintained within acceptable limits. Different droop functions in APC method was implemented and compared with the constant droop-based APC method. Changing droop value helps to decrease the energy loss by allowing the voltage to reside in the limits. An adaptive approach to adjust the droop values for overvoltage prevention with power curtailment minimization was proposed using ADP. The proposed method was able to maintain the voltage of the twelve houses in the upper boundary of the acceptable limits. The ADP based APC method reduced the energy loss in the system by 17.4%. The proposed technique reduced unnecessary PV curtailment and increased the PV power injection in the feeder.

4.2 Future work

SST models can be used in distribution networks for reactive power compensation for voltage regulation purposes with a view of enabling high intermittent renewable penetration. A yearly analysis of the ADP based APC method will be performed to evaluate its effectiveness. Also, the proposed technique will be examined under different

operating conditions to verify the robustness.

REFERENCES

[1] Renewable Energy Policy Network for the 21st century. (2016). *Renewables 2016 Global Status Report.* Accessed: May 31, 2017, [Online]. Available: http://www.ren21.net/wp-content/uploads/2016/06/GSR_2016_Full_Report.pdf.

[2] International Energy Agency. (2016). *Technology Roadmap Solar Photovoltaic Energy*. Accessed: Feb. 17, 2017, [Online]. Available: https://www.iea.org/publications/freepublications/publication/.

[3] National Renewable Energy Laboratory. (2012). Residential, commercial, and utility-scale photovoltaic (PV) system prices in the united states: Current drivers and cost-reduction opportunities. Accessed: Feb. 17, 2017, [Online]. Available: http://www.nrel.gov/docs/fy12osti/53347.pdf.

[4] National Renewable Energy Laboratory. (2016). *U.S. Solar Photovoltaic System Cost Benchmark: Q1 2016.* Accessed: Feb. 17, 2017, [Online]. Available: http://www.nrel.gov/news/press/2016/37745.

[5] Solar Energy Industries Associations. (2016). *Solar Market Insight Report 2016 Q4*, [Online]. Available: http://www.seia.org/research-resources/solar-market-insight-report-2016-q4.

[6] R. Tonkoski, D. Turcotte, and T. H. M. EL-Fouly, "Impact of high PV penetration on voltage profiles in residential neighborhoods," *IEEE Transactions on Sustainable Energy*, vol. 3, no. 3, pp. 518–527, Jul. 2012.

[7] P. P. Barker and R. W. D. Mello, "Determining the impact of distributed generation on power systems. I. Radial distribution systems," in *2000 Power Engineering Society Summer Meeting*, 2002, pp. 1645–1656.

[8] R. Tonkoski, L. A. C. Lopes, and T. H. M. El-Fouly, "Coordinated active power curtailment of grid connected PV inverters for overvoltage prevention," *IEEE Transactions on Sustainable Energy*, vol. 2, no. 2, pp. 139–147, Apr. 2011.

[9] *Standard for interconnecting distributed resources with electric power systems minutes*, Accessed: Nov. 4, 2016. [Online]. Available: https://http://grouper.ieee.org/groups/.

[10] X. Su, M. A. S. Masoum, and P. J. Wolfs, "Optimal PV inverter reactive power control and real power curtailment to improve performance of unbalanced four-wire LV distribution networks," *IEEE Transactions on Sustainable Energy*, vol. 5, no. 3, pp. 967–977, Jul. 2014.

[11] J. G. Kassakian and T. M. Jahns, "Evolving and emerging applications of power electronics in systems," *IEEE Journal of Emerging and Selected Topics in Power Electronics*, vol. 1, no. 2, pp. 47–58, Jun. 2013.

[12] D. Shah and M. L. Crow, "Online volt-var control for distribution systems with solid-state transformers," *IEEE Transactions on Power Delivery*, vol. 31, no. 1, pp. 343–350, Feb. 2016.

[13] Y. Jiang, L. Breazeale, R. Ayyanar, and X. Mao, "Simplified solid state transformer modeling for Real Time Digital Simulator (RTDS)," in *IEEE Energy Conversion Congress and Exposition (ECCE)*, 2012, pp. 1447–1452.

[14] V. Ramachandran, A. Kuvar, U. Singh, S. Bhattacharya, and M. Baran, "A system level study employing improved solid state transformer average models with renewable energy integration," in *2014 IEEE Power and Energy Society (PES) General Meeting — Conference Exposition*, 2014, pp. 1–5.

[15] X. Mao, S. Falcones, and R. Ayyanar, "Energy-based control design for a solid state transformer," in *IEEE Power and Energy Society (PES) General Meeting*, 2010, 7 pp.

[16] T. Zhao, J. Zeng, S. Bhattacharya, M. E. Baran, and A. Q. Huang, "An average model of solid state transformer for dynamic system simulation," in *IEEE Power and Energy Society (PES) General Meeting*, 2009, 8 pp.

[17] X. She, A. Q. Huang, F. Wang, and R. Burgos, "Wind energy system with integrated functions of active power transfer, reactive power compensation, and voltage conversion," *IEEE Transactions on Industrial Electronics*, vol. 60, no. 10, pp. 4512–4524, Oct. 2013.

[18] X. She, A. Q. Huang, and R. Burgos, "Review of solid-state transformer technologies and their application in power distribution systems," *IEEE Journal of Emerging and Selected Topics in Power Electronics*, vol. 1, no. 3, pp. 186–198, Sep. 2013.

[19] X. She, R. Burgos, G. Wang, F. Wang, and A. Q. Huang, "Review of solid state transformer in the distribution system: From components to field application," in *IEEE Energy Conversion Congress and Exposition (ECCE)*, 2012, pp. 4077–4084.

[20] S. Falcones, X. Mao, and R. Ayyanar, "Topology comparison for solid state transformer implementation," in *IEEE Power and Energy Society (PES) General Meeting*, 2010, 8 pp.

[21] A. Q. Huang, M. L. Crow, G. T. Heydt, J. P. Zheng, and S. J. Dale, "The future renewable electric energy delivery and management (FREEDM) system: The energy internet," *Proceedings of the IEEE*, vol. 99, no. 1, pp. 133–148, Jan. 2011.

[22] K. Stefanski, H. Qin, B. H. Chowdhury, J. W. Kimball, and S. Bhattacharya, "Identifying techniques, topologies and features for maximizing the efficiency of a distribution grid with solid state power devices," in *North American Power Symposium (NAPS)*, 2010, 7 pp.

[23] M Begović, A Pregelj, A Rohatgi, and D Novosel, "Impact of renewable distributed generation on power systems," in *Proceedings of the 34th Hawaii International Conference on System Sciences*, 2001, pp. 2001–2008.

[24] R. A. Walling, R. Saint, R. C. Dugan, J. Burke, and L. A. Kojovic, "Summary of distributed resources impact on power delivery systems," *IEEE Transactions on Power Delivery*, vol. 23, no. 3, pp. 1636–1644, Jul. 2008.

[25] R. C. Dugan, M. F. McGranaghan, and H. W. Beaty, "Electrical power systems quality," *McGraw-Hill, New York, NY*, 1996.

[26] *American national standard for electric power systems and equipment*, ANSI Standard C84.1, 2011.

[27] B. Poudel, "Overvoltage prevention in low voltage rural distribution network with high penetration of wind energy," Master's thesis, Department of Electrical Engineering and Computer Science, South Dakota State University, 2014.

[28] M. Juamperez, G. Yang, and S. B. Kjær, "Voltage regulation in LV grids by coordinated volt-var control strategies," *Journal of Modern Power Systems and Clean Energy*, vol. 2, no. 4, pp. 319–328, 2014.

[29] R. Kabiri, D. G. Holmes, B. P. McGrath, and L. G. Meegahapola, "LV grid voltage regulation using transformer electronic tap changing, with PV inverter reactive power injection," *IEEE Journal of Emerging and Selected Topics in Power Electronics*, vol. 3, no. 4, pp. 1182–1192, Dec. 2015.

[30] D. Wu, F. Tang, T. Dragicevic, J. C. Vasquez, and J. M. Guerrero, "Autonomous active power control for islanded ac microgrids with photovoltaic generation and energy storage system," *IEEE Transactions on Energy Conversion*, vol. 29, no. 4, pp. 882–892, Dec. 2014.

[31] M. A. Ghasemi and M. Parniani, "Prevention of distribution network overvoltage by adaptive droop-based active and reactive power control of PV systems," *Electric Power Systems Research*, vol. 133, pp. 313–327, Apr. 2016.

[32] F. Olivier, P. Aristidou, D. Ernst, and T. V. Cutsem, "Active management of low-voltage networks for mitigating overvoltages due to photovoltaic units," *IEEE Transactions on Smart Grid*, vol. 7, no. 2, pp. 926–936, Mar. 2016.

[33] S. Ghosh, S. Rahman, and M. Pipattanasomporn, "Distribution voltage regulation through active power curtailment with PV inverters and solar generation forecasts," *IEEE Transactions on Sustainable Energy*, vol. 8, no. 1, pp. 13–22, Jan. 2017.

[34] S. Chalise, H. R. Atia, B. Poudel, and R. Tonkoski, "Impact of active power curtailment of wind turbines connected to residential feeders for overvoltage prevention," *IEEE Transactions on Sustainable Energy*, vol. 7, no. 2, pp. 471–479, Apr. 2016.

[35] Y. Wang, P. Zhang, W. Li, W. Xiao, and A. Abdollahi, "Online overvoltage prevention control of photovoltaic generators in microgrids," *IEEE Transactions on Smart Grid*, vol. 3, no. 4, pp. 2071–2078, 2012.

[36] S. Alyami, Y. Wang, C. Wang, J. Zhao, and B. Zhao, "Adaptive real power capping method for fair overvoltage regulation of distribution networks with high penetration of PV systems," *IEEE Transactions on Smart Grid*, vol. 5, no. 6, pp. 2729–2738, Nov. 2014.

[37] J. Si and Y.-T. Wang, "Online learning control by association and reinforcement," *IEEE Transactions on Neural Networks*, vol. 12, no. 2, pp. 264–276, Mar. 2001.

[38] D. Shrestha, U. Tamrakar, N. Malla, Z. Ni, and R. Tonkoski, "Reduction of energy consumption of virtual synchronous machine using supplementary adaptive dynamic programming," in *2016 IEEE International Conference on Electro Information Technology (EIT)*, 2016, pp. 0690–0694.

[39] N. Malla, D. Shrestha, Z. Ni, and R. Tonkoski, "Supplementary control for virtual synchronous machine based on adaptive dynamic programming," in *2016 IEEE Congress on Evolutionary Computation (CEC)*, 2016, pp. 1998–2005.

[40] W. Guo, F. Liu, J. Si, D. He, R. Harley, and S. Mei, "Online supplementary ADP learning controller design and application to power system frequency control with large-scale wind energy integration," *IEEE Transactions on Neural Networks and Learning Systems*, vol. 27, no. 8, pp. 1748–1761, Aug. 2016.

[41] Y. Tang, H. He, Z. Ni, J. Wen, and X. Sui, "Reactive power control of grid-connected wind farm based on adaptive dynamic programming," *Neurocomputing*, vol. 125, pp. 125–133, 2014.

[42] Z. Ni, H. He, and J. Wen, "Adaptive learning in tracking control based on the dual critic network design," *IEEE Transactions on Neural Networks and Learning Systems*, vol. 24, no. 6, pp. 913–928, Jun. 2013.

[43] N. Malla, U. Tamrakar, D. Shrestha, Z. Ni, and R. Tonkoski, "Online learning control for harmonics reduction based on current controlled voltage source power inverters," *IEEE/CCA Journal of Automatica Sinica*, 2017, accepted, to appear.

[44] R. Tonkoski and L. A. C. Lopes, "Voltage regulation in radial distribution feeders with high penetration of photovoltaic," in *2008 IEEE Energy 2030 Conference*, 2008, 7 pp.

[45] H. R. Atia, A. Shakya, P. Tandukar, U. Tamrakar, T. M. Hansen, and R. Tonkoski, "Efficiency analysis of ac coupled and dc coupled microgrids considering load profile variations," in *2016 IEEE International Conference on Electro Information Technology (EIT)*, 2016, pp. 0695–0699.

[46] T. Hansen, E. Chong, S. Suryanarayanan, A. Maciejewski, and H. Siegel, "A partially observable markov decision process approach to residential home energy management," *IEEE Transactions on Smart Grid*, 11 pp., Jun. 2016, to appear.